Supplementary Information (SI) for Chemical Science.
This journal is © The Royal Society of Chemistry 2025

Supplemental Information

3D Printable Organic Room-Temperature Phosphorescent Materials and Printed Real-Time Sensing and Display Devices

Haodong Sun, Yuxin Xiao, Yunfei He, Xiaoyu Wei, Jindou Zou, Yuanda Luo, Yazhang Wu, Jiaxin Zhao, Vonika Ka-Man Au and Tao Yu

Additional experimental details

Reagents and materials

3,6-dibromo-9-phenyl-9H-carbazole, 3,6-dibromo-9H-carbazole, bromoethane, 9-phenyl-9H-carbazole, benzoyl chloride, 1,3-Diphenylisobenzofuran(DPBF), aluminium chloride ($AlCl_3$), potassium hydroxide (KOH) and potassium carbonate (K_2CO_3) were purchased from Shanghai Energy-Chemical Co. Ltd. and used without any further purification. Phenyl(4-(4,4,5,5-tetramethyl-1,3,2-dioxaborolan-2-yl)phenyl)methanone was synthesized according to our previous work.[1] Tetrakis(triphenylphosphine)palladium ($Pd(PPh_3)_4$) was synthesized by our group. Poly(methyl methacrylate) (PMMA, average molecular weight ~200,000) were also purchased from Shanghai Energy-Chemical Co. Ltd. The 3D printed resin used in digital light process (DLP) 3D printing was purchased from Time 80s.

Synthesis and Characterization of Final Compounds

Measurements

^1H NMR spectra were performed with on a Bruker AVANCE NEO 500 Nuclear Magnetic Resonance Spectrometer ((500 MHz)) in $CDCl_3$ using tetramethylsilane (TMS) as the internal standard. High Resolution ESI mass spectra were collected from a MAT95XP-HRM spectrometer. High-performance liquid chromatography (HPLC) was performed on an UltiMate 3000 (Thermo Fisher Scientific). UV-vis absorption spectra of solutions were performed on a Hitachi U-3900 spectrophotometer. The steady emission and delayed emission spectra were tested on Edinburgh steady-transient fluorescence spectrometer (FLS-1000) equipped with a white light source and laser light sources (280 and 365 nm). The afterglow emissions of EtCzBP@PMMA at Fig. S32-S33 were measured by a Shimadzu RF-5301 PC spectrometer or an Ocean Optics Maya Pro2000 with 310 nm and 365nm Rhinospectrum RhinoLED as the excitation source. Absolute PL quantum yields were

measured using a Hamamatsu absolute PL quantum yield spectrometer (C11347-11 Quantaurus-QY). Optical microscopy and laser scanning confocal microscopy (LSCM) were tested on Laser confocal microscopy system (C2+&N-SIM E, Nikon Instruments Inc.). The layer thickness upon each exposure polymer films was tested on YongXin NIB 610 (Guona Chenyu Technology Co., Ltd). Single-crystal analyses of EtCzBP and PhCzBP were determined using Bruker D8 Quest X-ray Single Crystal Diffractometer with a (Cu) X-ray source. The transmission of the films was also measured on Hitachi U-3900 and used an empty glass substrate and colorimetric dish as reference. Optical photographs and videos of the films and applications were shot by a Sony LICE-6400M camera. The infrared images of temperature distribution for the 3D printing materials and devices were obtained from the infrared imager (FOTRIC 323 Infrared Cameras). The intensity of UV light (365 nm) was obtained from the ultraviolet radiation meter (TENMARS TM-213).

Test environment

Unless other noted, all photophysical properties of the films were collected at 298 K with relative humidity (RH) of ~30% in air.

General procedures for synthesis of phosphorescence emitters

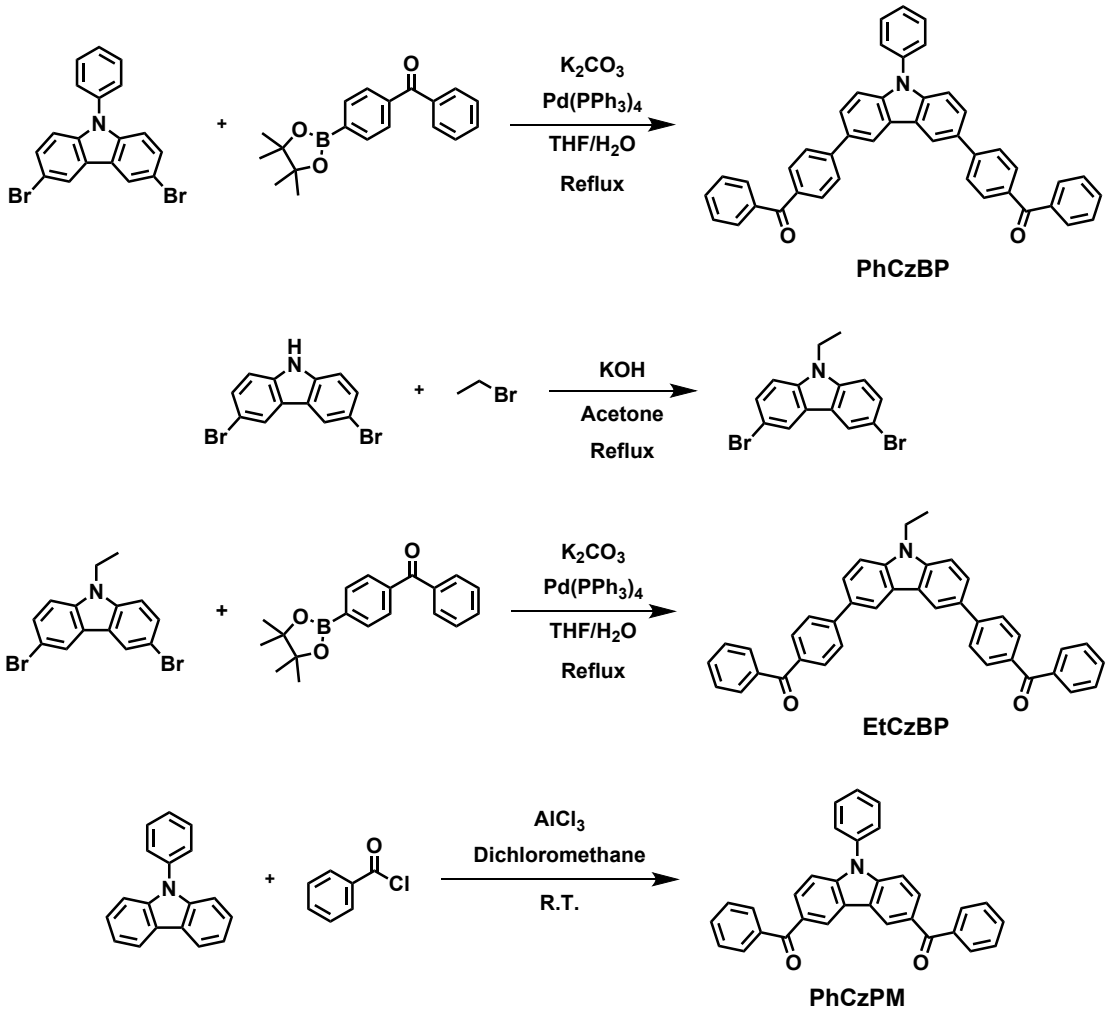

Fig. S1. The details for the synthetic routes of phosphors EtCzBr, PhCzBr, EtCzBP, PhCzBP and PhCzPM were listed.

((9-phenyl-9H-carbazole-3,6-diyl)bis(4,1-phenylene))bis(phenylmethanone) (PhCzBP). 3,6-dibromo-9-phenyl-9H-carbazole (1.50 g, 3.74 mmol), phenyl(4-(4,4,5,5-tetramethyl-1,3,2-dioxaborolan-2-yl)phenyl)methanone (2.77 g, 8.98 mmol), K_2CO_3 (3.10 g, 22.44 mmol) and $Pd(PPh_3)_4$ (0.21 g, 0.187 mmol) were added to a dried flask (250 mL) filled with mixed solution of tetrahydrofuran (21 mL) and deionized water (7 mL) under argon atmosphere. The mixture was heated up to reflux temperature and stirred for 18 h. After cooling to room temperature, the mixed solution was distilled out to obtain dry solid. The dry solid was dissolved in

dichloromethane and washed with brine. After removal of the solvents of the organic layer, the crude products were purified by silica-gel chromatography with dichloromethane/n-hexane (1/1, v /v) to give PhCzBP (0.90 g, 39.86 %). ^{1}H NMR (500 MHz, Chloroform-*d*), (TMS, ppm): δ = 8.50 (s, 2H), 7.95 (d, *J* = 8.1 Hz, 4H), 7.87 (td, *J* = 5.3, 2.6 Hz, 8H), 7.76 (d, *J* = 8.6 Hz, 2H), 7.67 (t, *J* = 7.7 Hz, 2H), 7.65 – 7.59 (m, 4H), 7.53 (q, *J* = 7.6 Hz, 7H). ^{13}C NMR (126 MHz, Chloroform-*d*) δ 196.37, 145.88, 141.40, 137.96, 135.60, 132.41, 132.34, 130.94, 130.13, 130.04, 128.34, 126.98, 125.90, 124.08, 119.26, 110.58. High-Resolution ESI-MS (Fig. S2) m/z calcd for $[C_{44}H_{29}NO_2, M+H]^+$, 604.2271; found: 604.2273.

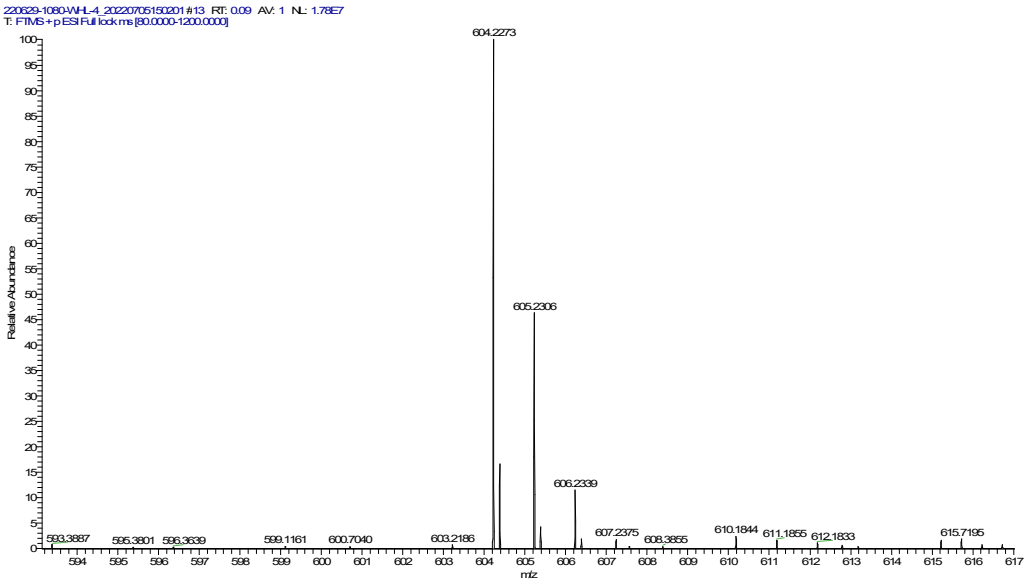

Fig. S2. High-Resolution ESI mass spectrum of PhCzBP.

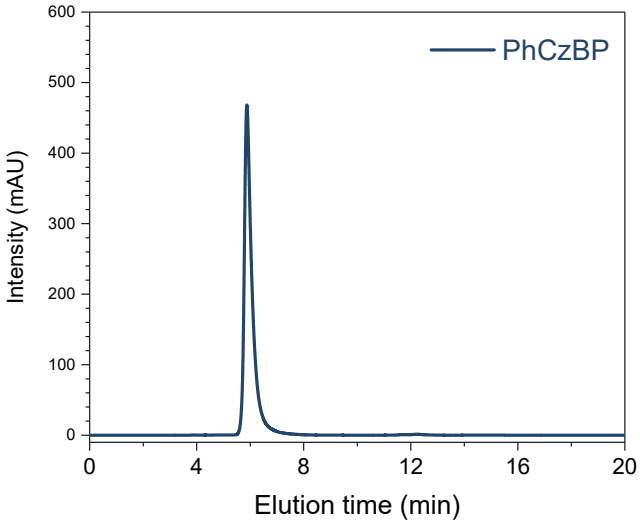

Fig. S3. HPLC spectrum of PhCzBP recorded at 254 nm with methanol as eluent.

((9-ethyl-9H-carbazole-3,6-diyl)bis(4,1-phenylene))bis(phenylmethanone) (EtCzBP). 3,6-dibromo-9H-carbazole (3.00 g, 9.23 mmol), bromoethane (1.06 g, 9.69 mmol), and KOH (3.00 g, 13.85 mmol) were added to a dried flask (250 mL) filled with acetone (30 mL) under ambient conditions. The mixture was heated up to reflux temperature and stirred for 18 h. After cooling to room temperature, the mixed solution was distilled out to obtain dry solid.[2] The dry solid was dissolved in dichloromethane and washed with brine. After removal of the solvents of the organic layer, the crude products were purified by silica-gel chromatography with dichloromethane/n-hexane (1/10, v /v) to give 3,6-dibromo-9-ethyl-9H-carbazole (2.23 g, 68.43 %). The synthetic procedure of EtCzBP was identical to that of PhCzBP, (0.31 g, 66.85 %). ^{1}H NMR (500 MHz, Chloroform-*d*), (TMS, ppm): δ = 8.49 (s, 2H), 7.97 (d, 4H), 7.89 (t, 8H), 7.85 (d, *J* = 8.5, 2H), 7.63 (t, 2H), 7.59 – 7.52 (m, 6H), 4.49 (q, *J* = 7.2 Hz, 2H), 1.55 (t, 3H). ^{13}C NMR (126 MHz, Chloroform-*d*) δ 195.28, 136.89, 134.32, 131.21, 130.14, 129.83, 128.94, 128.92, 127.23, 125.79, 124.50, 118.26, 108.16, 36.82, 12.85. High-Resolution ESI-MS (Fig. S3) m/z calcd for $[C_{40}H_{29}NO_2, M+H]^+$, 556.2271; found: 556.2273.

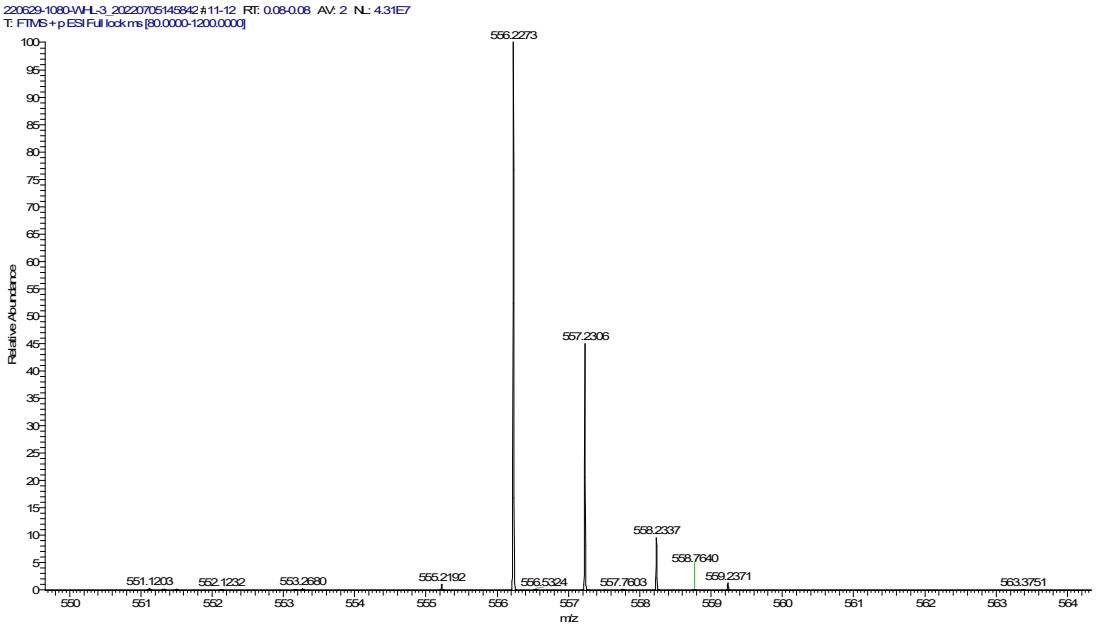

Fig. S4. High-Resolution ESI mass spectrum of EtCzBP.

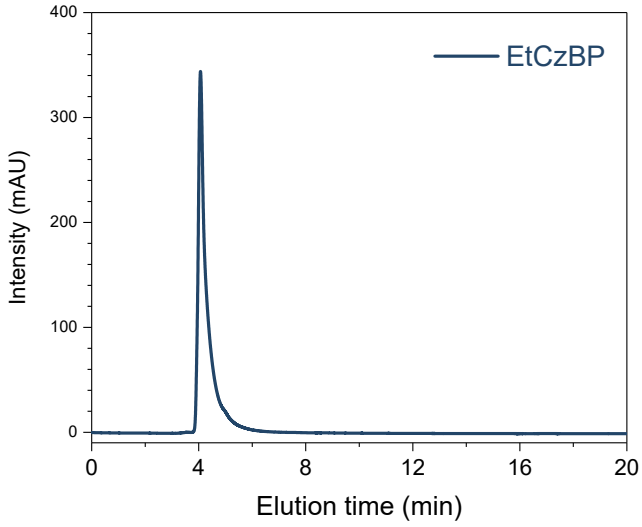

Fig. S5. HPLC spectrum of EtCzBP recorded at 254 nm with methanol as eluent.

Synthetic details of (9-phenyl-9H-carbazole-3,6-diyl)bis(phenylmethanone) (PhCzPM). The synthetic route of PhCzPM was shown in Scheme S3. A stirred mixture of 9-phenyl-9H-carbazole (1.00 g, 4.11 mmol) and benzoyl chloride (1.16 g, 8.22 mmol) in dichloromethane (30 mL) was treated by slow addition of $AlCl_3$ (3.29 g, 24.66 mmol) under argon atmosphere. The mixture was stirred at room temperature for 6 h. After the reaction was completed, cold water was added to the reaction until no bubbles were formed. The mixture was then extracted with dichloromethane (3 × 50 mL). After removal of the solvents of the organic layer, the crude products were purified by silica-gel chromatography with dichloromethane/n-hexane (1/1, v /v) to give PhCzPM (0.84 g, 45.16%). ^{1}H NMR (500 MHz, Chloroform-*d*), (TMS, ppm): δ = 8.67 (d, 2H), 8.03 (d, *J* = 8.6Hz, 2H), 7.87 (d, 4H), 7.71 (t, *J* = 7.8 Hz, 2H), 7.66 – 7.58 (m, 5H), 7.55 (t, *J* = 7.6 Hz, 4H), 7.48 (d, *J* = 8.6 Hz, 2H). ^{13}C NMR (126 MHz, Chloroform-*d*) 195.36, 143.18, 137.48, 135.29, 131.02, 129.49, 129.27, 129.12, 128.93, 128.24, 127.69, 127.30, 126.12, 122.99, 122.02, 108.96, 76.25, 75.99, 75.74. High-Resolution ESI-MS (Fig. S4) m/z calcd for $[C_{32}H_{21}NO_2, M+H]^+$, 452.1645; found: 452.1647.

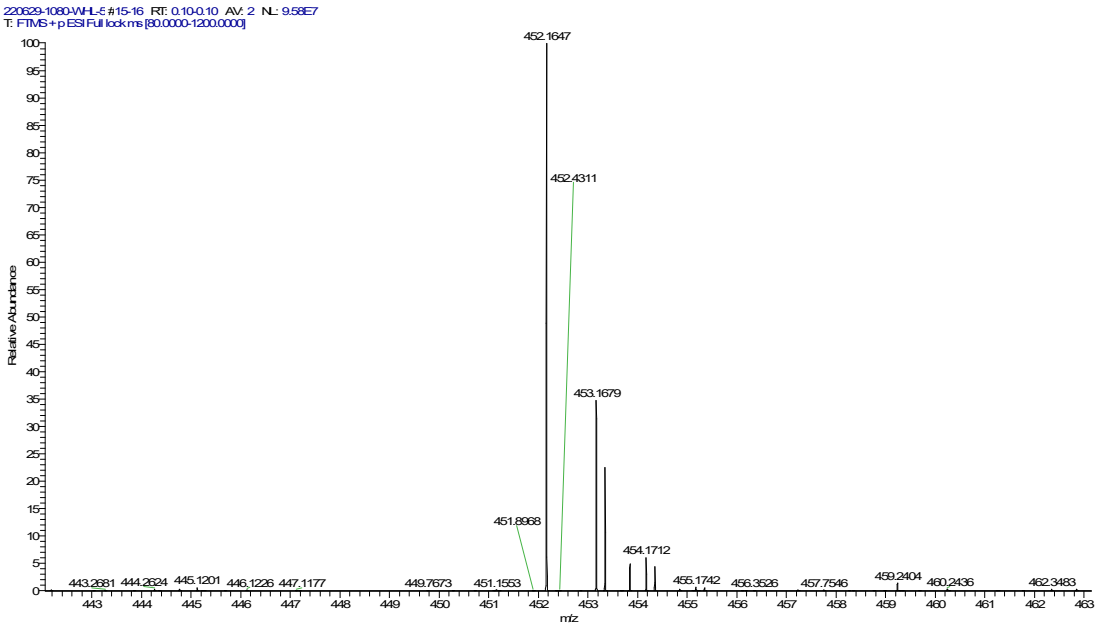

Fig. S6. High-Resolution ESI mass spectrum of PhCzPM.

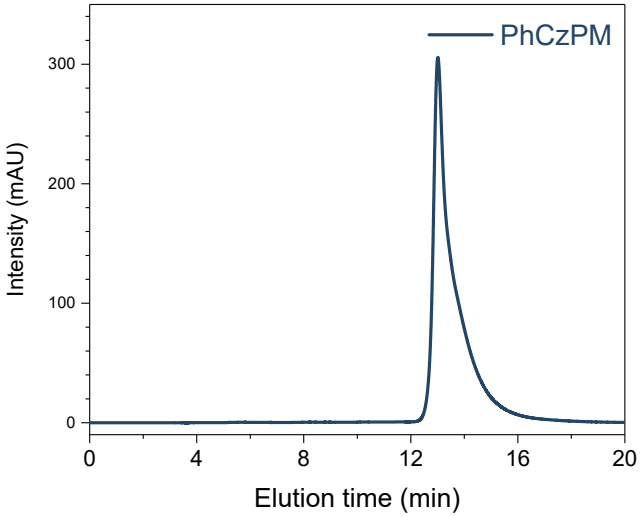

Fig. S7. HPLC spectrum of PhCzPM recorded at 254 nm with methanol: water as eluent in ratios of 90:10 (v/v).

Film preparation

PMMA solution (100mg/mL): PMMA (2 g) and tetrahydrofuran (THF, 20 mL) solvent were mixed in a flask and stirred for 24 hours at room temperature until the PMMA particles completely dissolved. The clear PMMA/THF solution was used for the subsequent film fabrication.

Mixed EtCzBP (5 mg), PhCzBP (5 mg), or PhCzPM (5 mg) in PMMA/THF solution (5 mL) at a vessel. The mixture was ultrasonicated for 1 h and then the mixture (1 mL) was dropped onto a glass substrate (3 cm× 3 cm). After evaporation of the solvent, the films were placed in a drying oven at 70 °C for 6 h. Then the EtCzBP@PMMA, PhCzBP@PMMA and PhCzPM@PMMA films with a mass ratio of 5 wt% were obtained.

Singlet oxygen detection

1,3-Diphenylisobenzofuran (DPBF) was used as a detector to monitor the production of singlet oxygen. A solution of DPBF and a mixed solution of EtCzBP&DPBF at a concentration of 1.0×10^{-5} M in N,N-Dimethylformamide (DMF) were prepared. The decomposition of DPBF was examined by recording the absorbance at 415 nm at various irradiation times, an UV light (365 nm) was employed as the irradiation source.[3-5]

3D printing structure preparation

The 3D printed resin consists of methyl methacrylate (MMA, 40 wt%), tert-Butyl acrylate (t-BA, 40 wt%), aliphatic urethane diacrylate (AUD 20 wt%), and the photoinitiator, 2,4,6-trimethylbenzoyldiphenyl phosphine oxide (TPO, 1.5 wt%).

3D structures were fabricated using a commercial Digital Light Processing (DLP) 3D printer (nanoArch P150, BMF Material, China) equipped with a 405 nm light source. The model underwent processing using 3Dmax software, followed by slicing of the STL file using BMF slice software to generate 2D images (1920 × 1080) with a thickness of 50 μm. Throughout the printing process, an exposure intensity of 9.2 mW/cm² and an exposure time per layer of 3 seconds were maintained. After printing, the printed structures underwent post-processing involving ultrasonic cleaning with ethanol to remove residual resin, followed by curing in a photocuring oven (405 nm, BMF G2, China) at room temperature for 1 hour.

Thermotic calculation details

The molecular geometry optimization and excitation energy calculation of EtCzBP, PhCzBP, and PhCzPM were realized by density function theory (DFT) and time-dependent DFT, respectively. The calculation process was performed in Gaussian 09 program at the B3LYP/6-311G* level.[6, 7] Spin-orbital couplings (SOC) constants between the singlet and triplet excited states were calculated via ORCA 4.2.1 at B3LYP/6-311G* level.[8] The electron and hole analysis of the specific energy level was performed with Multiwfn 3.8 code.[9, 10] The isosurface maps of electron and hole distribution were rendered by Visual Molecular Dynamics (VMD) software (version 1.9.3).[11]

Supplementary Fig.s

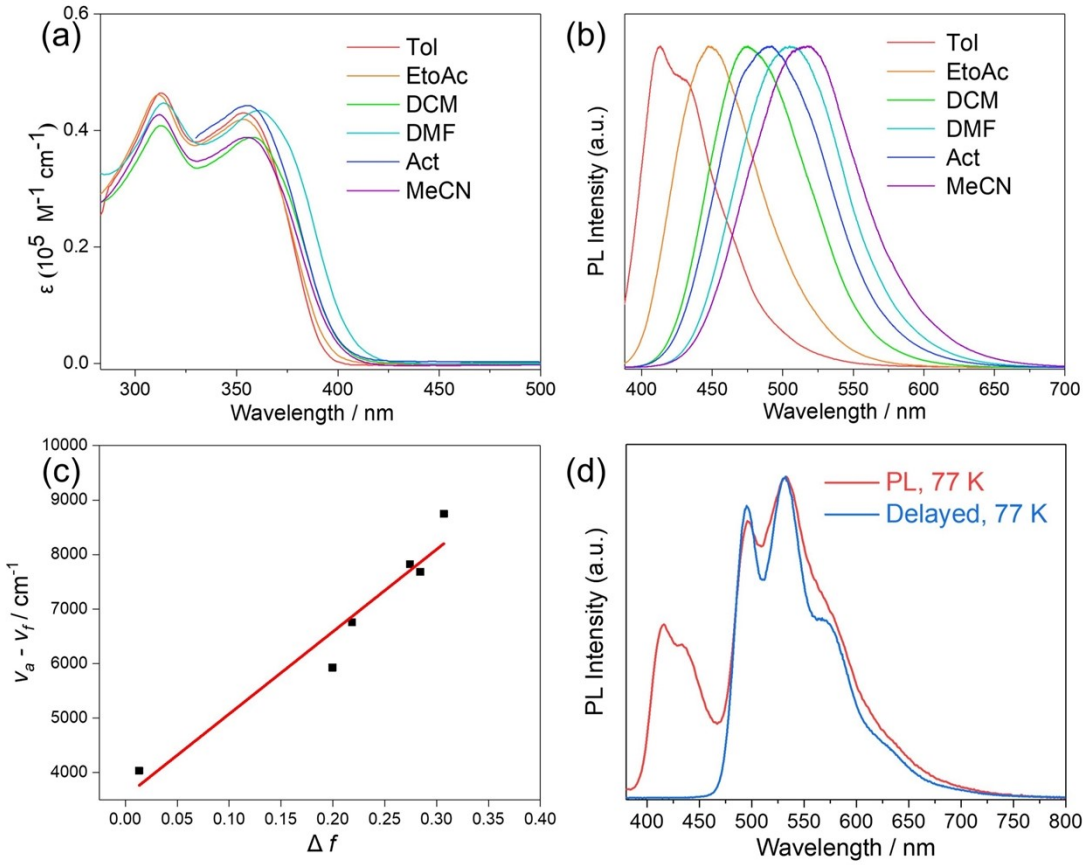

Fig. S8. The photophysical properties of EtCzBP in dilute solutions. (a) The UV-Vis absorption spectra in different solvents with concentration of 1.0×10^{-5} mol/L. (Tol:

toluene, EtoAc: ethyl acetate, DCM:dichloromethane, DMF: dimethylformamide, Act:a cetone) (b) The steady-state PL spectra of EtCzBP in different solvents with concentration of 1.0×10^{-5} mol/L. (c) Lippert-Mataga of EtCzBP in solvents of increasing polarity. The slope for the fit is 3565 cm^{-1} (R^2 = 0.94). (d) The steady-state PL spectrum and delayed spectrum (delayed time = 8 ms) of EtCzBP in 2-MeTHF solvents (1.0×10^{-5} mol/L) at 77 K.

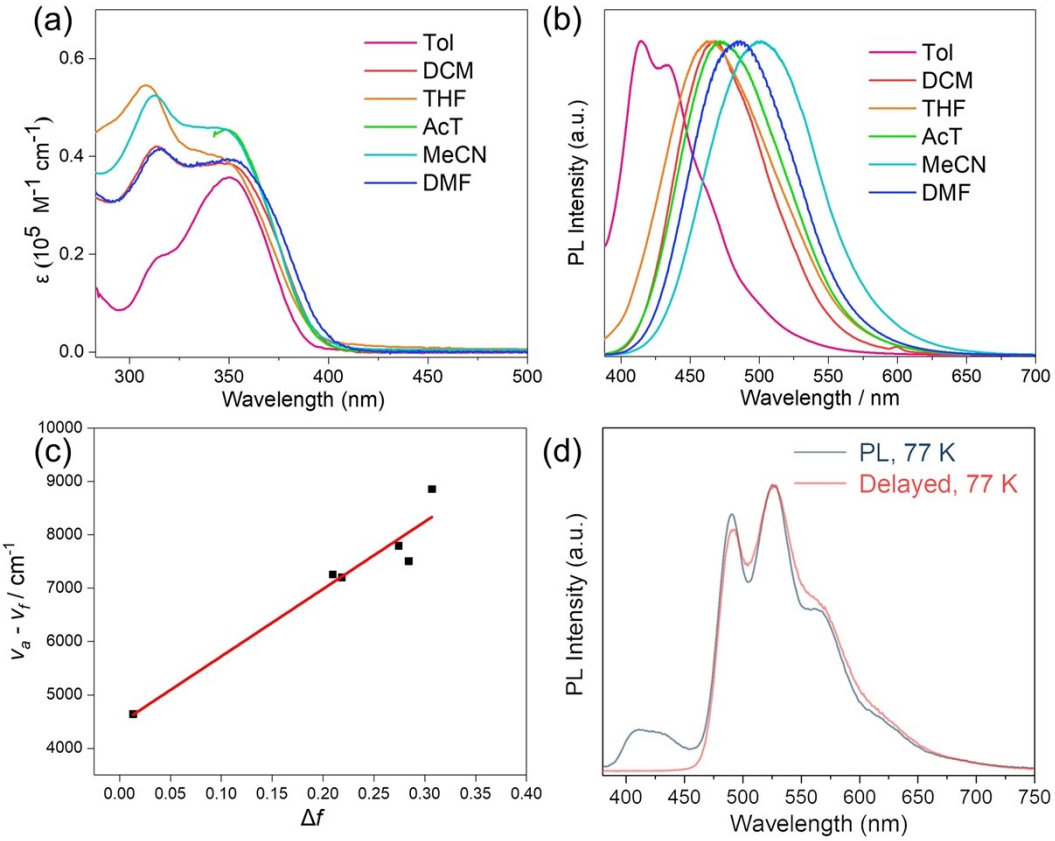

Fig. S9. The photophysical properties of PhCzBP in dilute solutions. (a) The UV-Vis absorption spectra in different solvents with concentration of 1.0×10^{-5} mol/L. (THF: Tetrahydrofuran)(b) The steady-state PL spectra of PhCzBP in different solvents with concentration of 1.0×10^{-5} mol/L. (c) Lippert-Mataga of PhCzBP in solvents of increasing polarity. The slope for the fit is 4462 cm^{-1} (R^2 = 0.94).(d) The steady-state PL spectrum and delayed spectrum (delayed time = 8 ms) of PhCzBP in 2-MeTHF solvents (1.0×10^{-5} mol/L) at 77 K.

Lippert-Mataga equation

According to the Lippert-Mataga equation as shown in below, where ε is the dielectric constant of the solvent, and n is the solvent's refractive index.

$$\Delta \mathrm{f} = \frac{\varepsilon - 1}{2\varepsilon + 1} - \frac{n^2 - 1}{2n^2 + 1}$$

According to the Lippert-Mataga method, the change in the dipole moment, Δμ, is a function of the solvent's polarizability, and the Stokes shift ($\Delta\nu_{st}$) as follows: where ν_A is the energy of the absorbance maximum in wavenumbers and ν_E is the energy of the emission maximum in wavenumbers.

$$\Delta\nu_{st} = \nu_A - \nu_E = \frac{2\Delta\mu^2}{hc\,\rho^3}\Delta \mathrm{f} + Constant$$

Table S1. Absorption maxima, emission maxima in various solvents for EtCzBP with the dielectric constant (ε) and the refractive index (n) of the solvent.

Solvent	$\lambda_{abs.}$	$\lambda_{f.}$	ν_a -ν_{em} (cm^{-1})	Δf	ε	n
n-Hexane	345	410	4595.2633	-0.0060	1.87	1.3840
TOL	354	413	4035.5125	0.0132	2.38	1.4969
EtoAc	354	448	5927.1590	0.1996	6.02	1.3724
DCM	359	474	6758.1068	0.2184	9.1	1.4244
AcT	356	490	7681.7244	0.2843	20.7	1.3588
DMF	362	505	7822.3292	0.2744	36.7	1.4305
MeCN	356	517	8747.5279	0.3070	38.8	1.3416

Table S2. Absorption maxima, emission maxima in various solvents for PhCzBP with the dielectric constant (ε) and the refractive index (n) of the solvent.

Solvent	$\lambda_{abs.}$	λ_f	ν_a -ν_f (cm^{-1})	Δf	ε	n
TOL	348	415	4639.246642	0.0132	2.38	1.4969
DCM	350	468	7203.907204	0.2184	9.1	1.4244

THF	346	462	7256.712459	0.2096	7.58	1.4072
AcT	348.5	472	7507.963913	0.2843	20.7	1.3588
MeCN	347	501	8858.363964	0.3070	38.8	1.3416
DMF	352.5	486	7792.662639	0.2744	36.7	1.4305

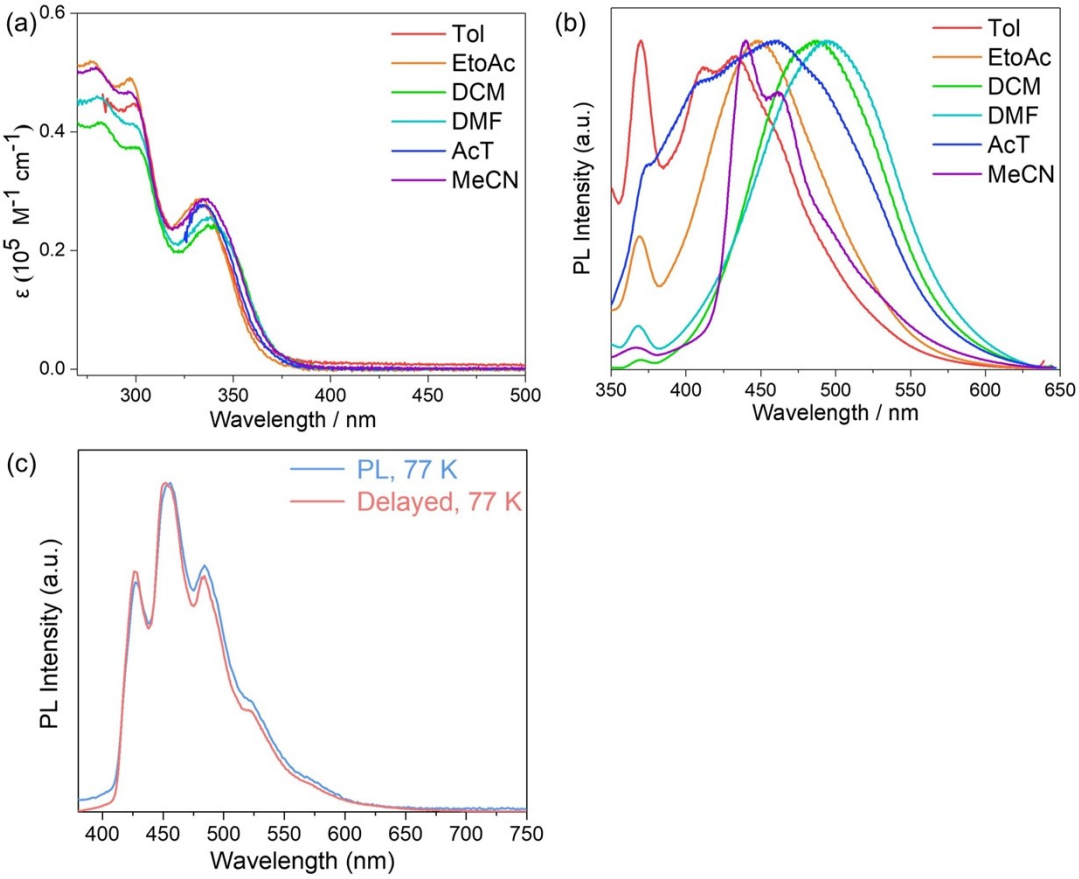

Fig. S10. The photophysical properties of PhCzPM in dilute solutions. (a) The UV-Vis absorption spectra in different solvents with concentration of 1.0×10^{-5} mol/L. (b) The steady-state PL spectra of PhCzPM in different solvents with concentration of 1.0×10^{-5} mol/L. (c) The steady-state PL spectrum and delayed spectrum (delayed time = 8 ms) of PhCzPM in 2-MeTHF solvents (1.0×10^{-5} mol/L) at 77 K.

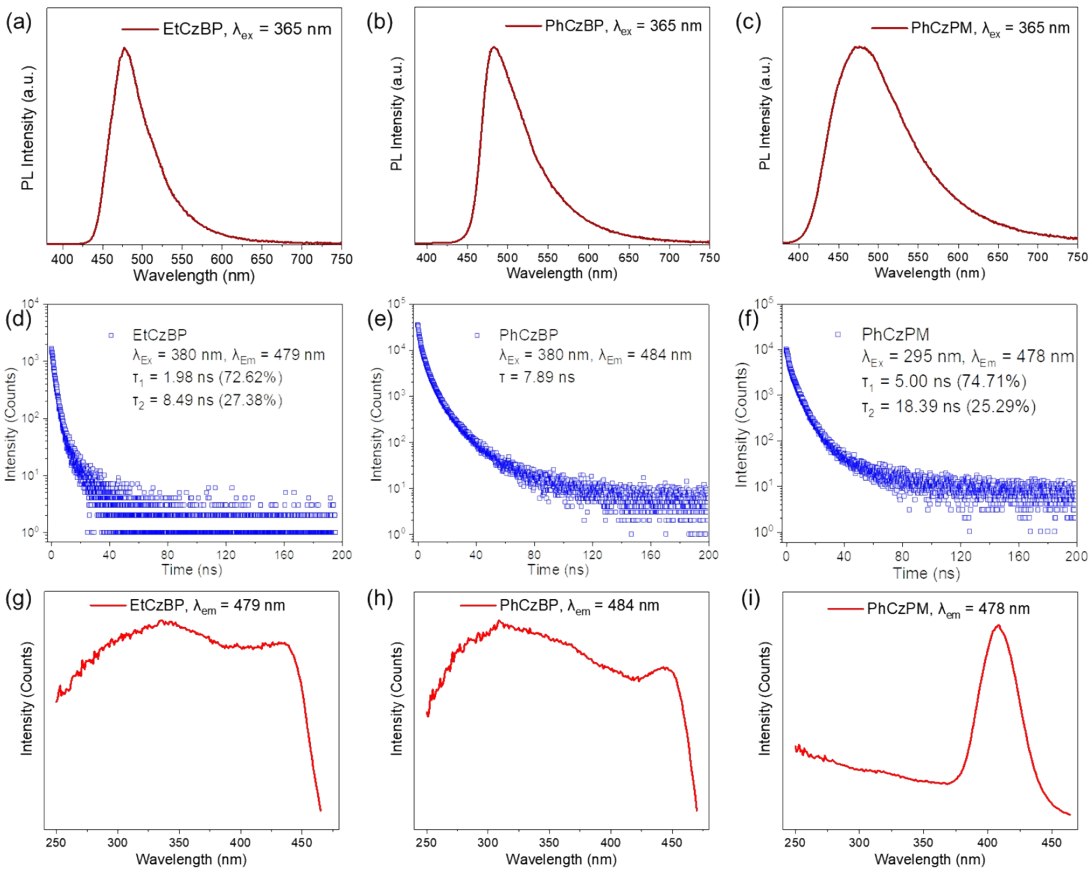

Fig. S11. The photophysical properties of crystalline EtCzBP, PhCzBP and PhCzPM. (a), (d) and (g) were the steady-state PL spectra, the time-resolved decay curves and excitation spectra for EtCzBP, respectively. (b), (e) and (h) were the steady-state PL spectra, the time-resolved decay curves and excitation spectra for PhCzBP, respectively. (c), (f) and (i) were the steady-state PL spectra, the time-resolved decay curves and excitation spectra for PhCzPM, respectively. (d, EtCzBP: τ_{int}=3.76±0.10 ns, X^2=1.07; PhCzBP: τ_{int}=7.89±0.25 ns, X^2=1.18; PhCzPM: τ_{int}=8.39±0.20 ns, X^2=1.23)

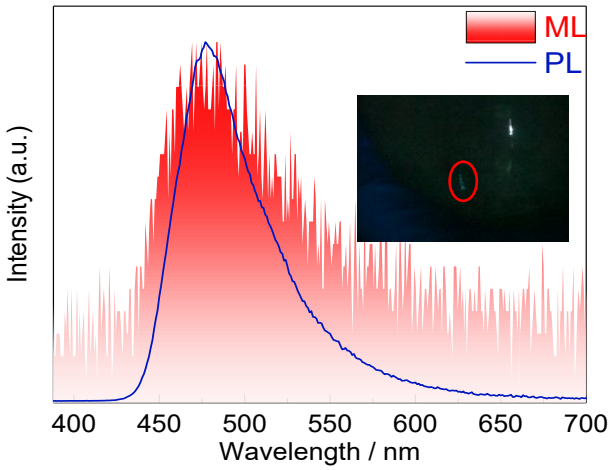

Fig. S12. Normalized PL and ML spectrum of crystalline EtCzBP at ambient conditions, inset: photograph of ML phenomenon generated by crushing EtCzBP in the dark with a scraper.

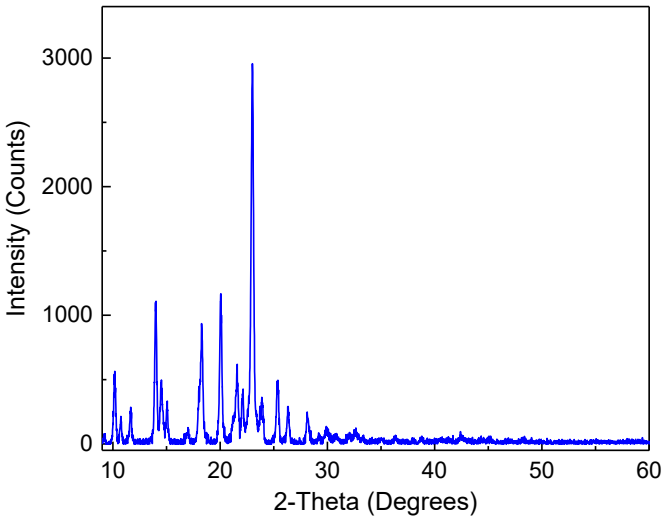

Fig. S13. XRD pattern of crystalline EtCzBP.

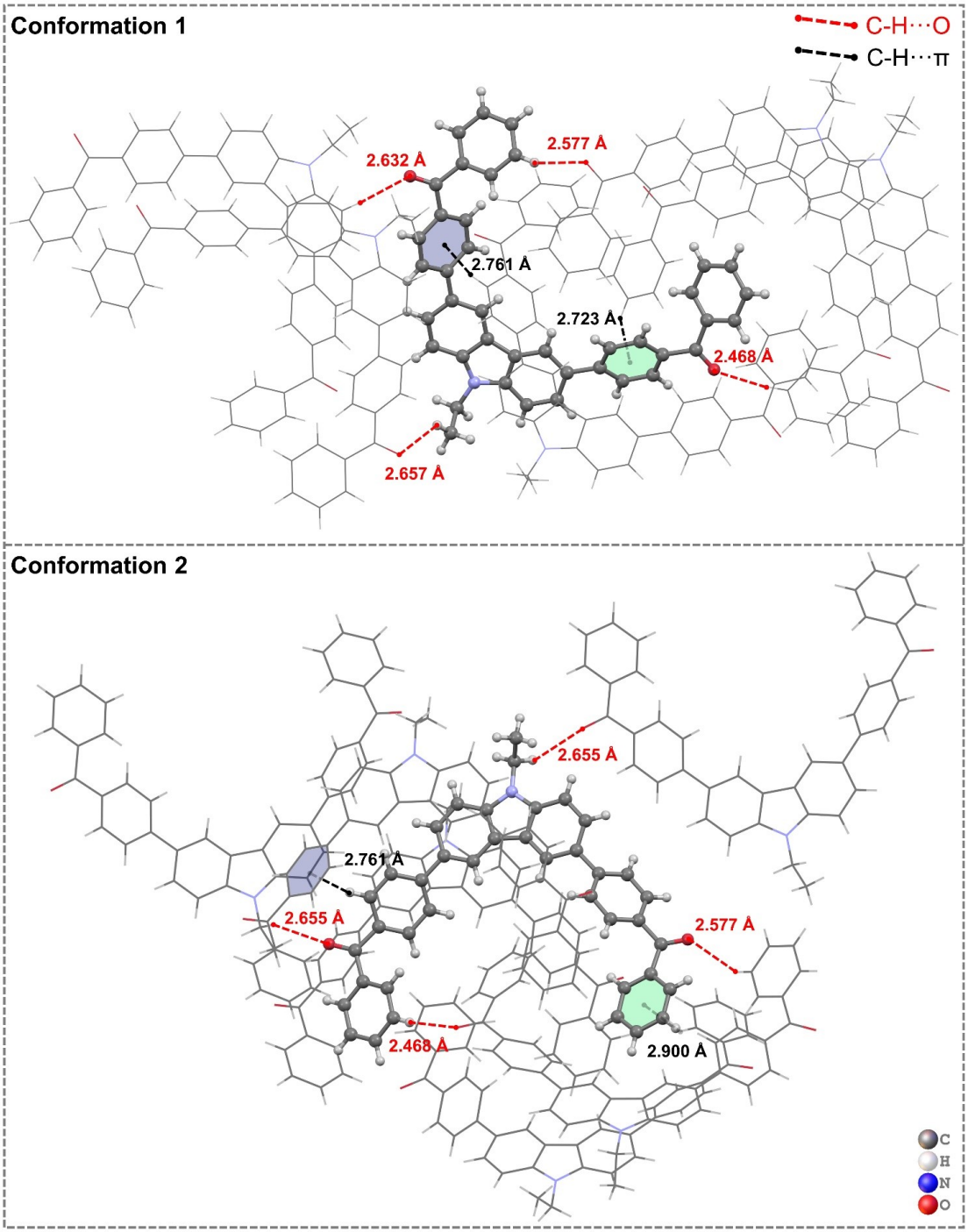

Fig. S14. Different intermolecular interactions in the single crystal of EtCzBP (CCDC 2189250).

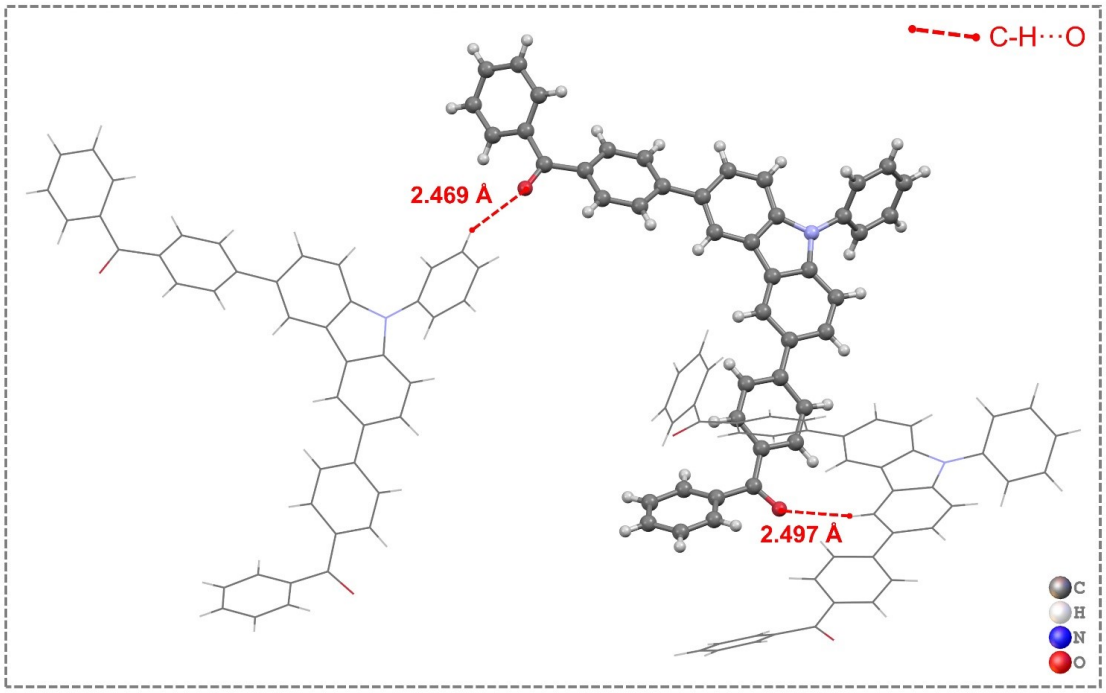

Fig. S15. Different intermolecular interactions in the single crystal of PhCzBP (CCDC 2299673).

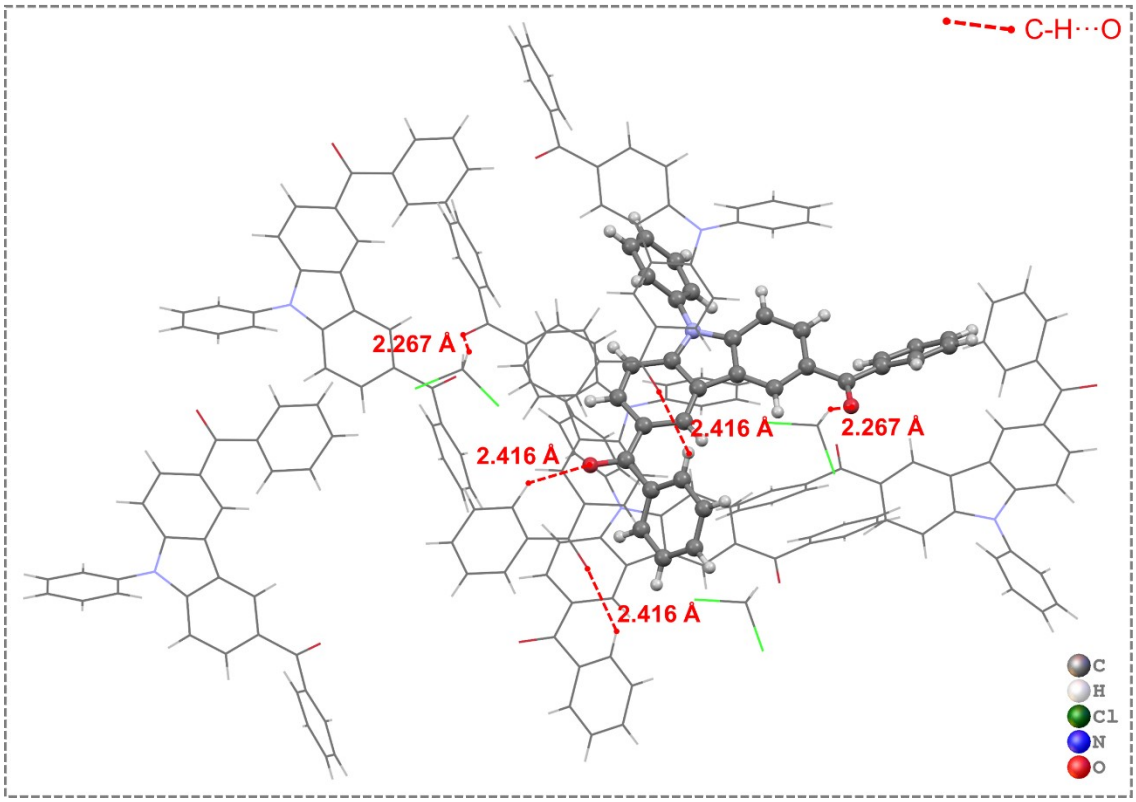

Fig. S16. Different intermolecular interactions in the single crystal of PhCzPM (CCDC 2341195).

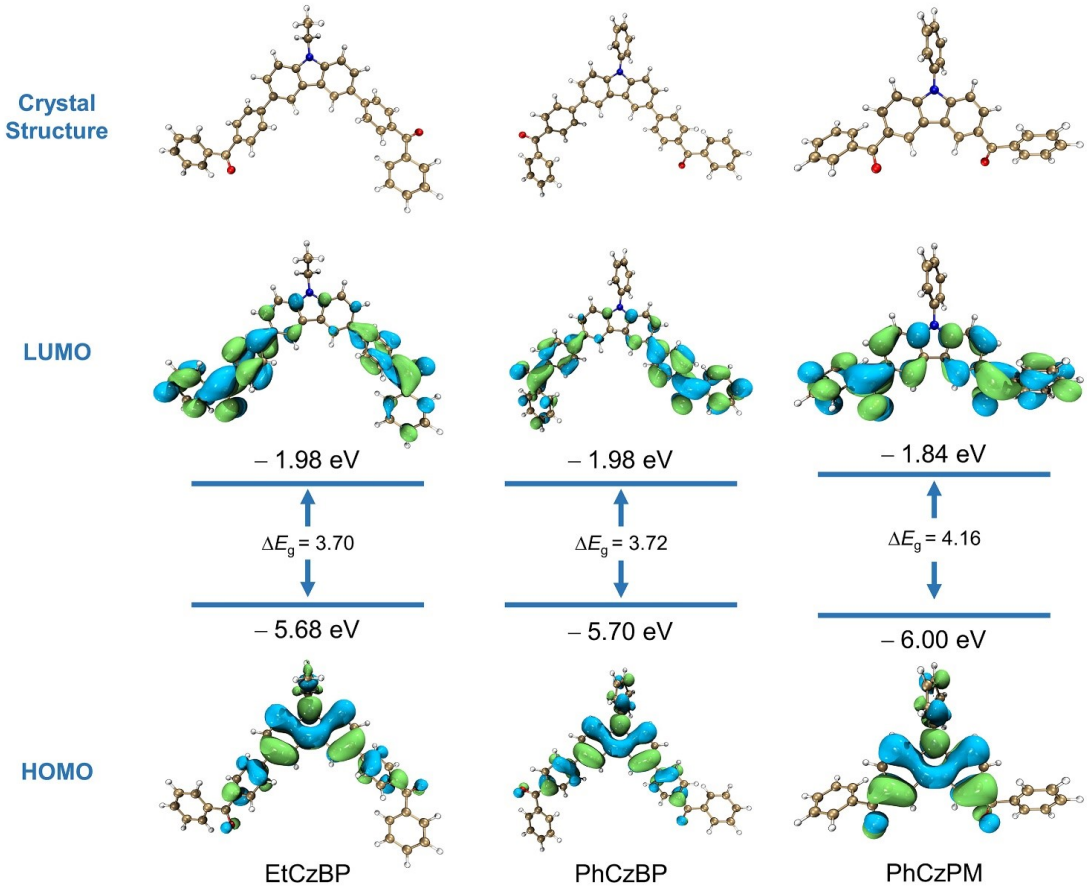

Fig. S17. The highest occupied molecular orbitals (HOMO) and the lowest unoccupied molecular orbitals (LUMO) density maps of EtCzBP, PhCzBP and PhCzPM. (Calculated at the B3LYP/6-311G* level, isovalue = 0.02)

Table S3 The energy levels and transition configurations of EtCzBP revealed by TD-DFT calculations.

Excited States	n-th	Energy (eV)	Transition configurations (%)
S_n	1	3.3012	H → L 94.5%
	2	3.4417	H → L+1 92.3%
T_n	1	2.7559	H → L 46.3%, H-2 → L+1 11.5%, H-3 → L 7.8%, H-1 → L+1 6.3%, H → L+3 6.2%
	2	2.8246	H → L+1 34.6%, H-2 → L 15.0%, H-1 → L 12.7%, H-3 → L+1 11.4%
	3	3.0505	H-3 → L 30.8%, H-4 → L+1 19.5%, H-2 → L+1 10.0%, H-1 → L+2 7.2%, H → L 5.2%
	4	3.0953	H-3 → L+1 22.0%, H-4 → L 20.9%, H → L+2 20.0%, H → L+1 10.4%
	5	3.1989	H → L+2 71.7%, H-4 → L 5.1%
	6	3.2749	H-1 → L+2 51.5%, H → L 10.2%, H-2 → L+2 9.5%

Table S4 The energy levels and transition configurations of PhCzBP revealed by TD-DFT calculations.

Excited States	n-th	Energy (eV)	Transition configurations (%)
S_n	1	3.3184	H → L 94.2%
	2	3.4409	H → L+1 91.7%
T_n	1	2.7665	H → L 43.5%, H-2 → L+1 12.3%, H-3 → L 8.8%, H-1 → L+1 6.6%, H → L+4 5.5%
	2	2.8266	H → L+1 33.7%, H-2 → L 14.6%, H-1 → L 12.4%, H-3 → L+1 11.6%
	3	3.0531	H-3 → L 29.6%, H-4 → L+1 19.4%, H-2 → L+1 9.4%, H-1 → L+2 6.6%, H → L 5.8%
	4	3.0961	H-3 → L+1 22.2%, H-4 → L 22.0%, H → L+2 13.4%, H → L+1 11.8%
	5	3.2330	H → L+2 77.0%
	6	3.2900	H-1 → L+2 49.5%, H → L 9.9%, H-2 → L+2 9.7%

Table S5 The energy levels and transition configurations of PhCzPM revealed by TD-DFT calculations.

Excited States	n-th	Energy (eV)	Transition configurations (%)
S_n	1	3.5840	H → L 54.9%, H-3 → L 17.0%, H-2 → L+1 14.8%
T_n	1	2.8793	H → L 51.1%, H-2 → L+1 14.5%, H-1 → L+2 10.7%, H-3 → L 9.4%
	2	3.0011	H-2 → L 39.9%, H → L+1 28.6%, H-3 → L+1 19.3%
	3	3.1897	H-3 → L 35.8%, H-2 → L+1 20.8%, H-1 → L+2 15.6%, H-8 → L+1 5.6%, H → L 5.2%
	4	3.2987	H → L+1 37.3%, H-3 → L+1 14.3%, H-2 → L 10.6%, H → L+2 10.2%, H-8 → L 8.9%
	5	3.4778	H-1 → L+2 38.7%, H → L 26.1%, H-1 → L+1 22.5%
	6	3.4897	H-1 → L 46.0%, H → L+2 33.8%
	7	3.5456	H-7 → L 31.1%, H-6 → L+1 25.4%, H-5 → L+7 8.3%, H-4 → L+6 5.7%
	8	3.5525	H-6 → L 25.3%, H-7 → L+1 22.0%, H → L+2 10.0%, H-4 → L+7 7.6%, H-5 → L+6 5.7%

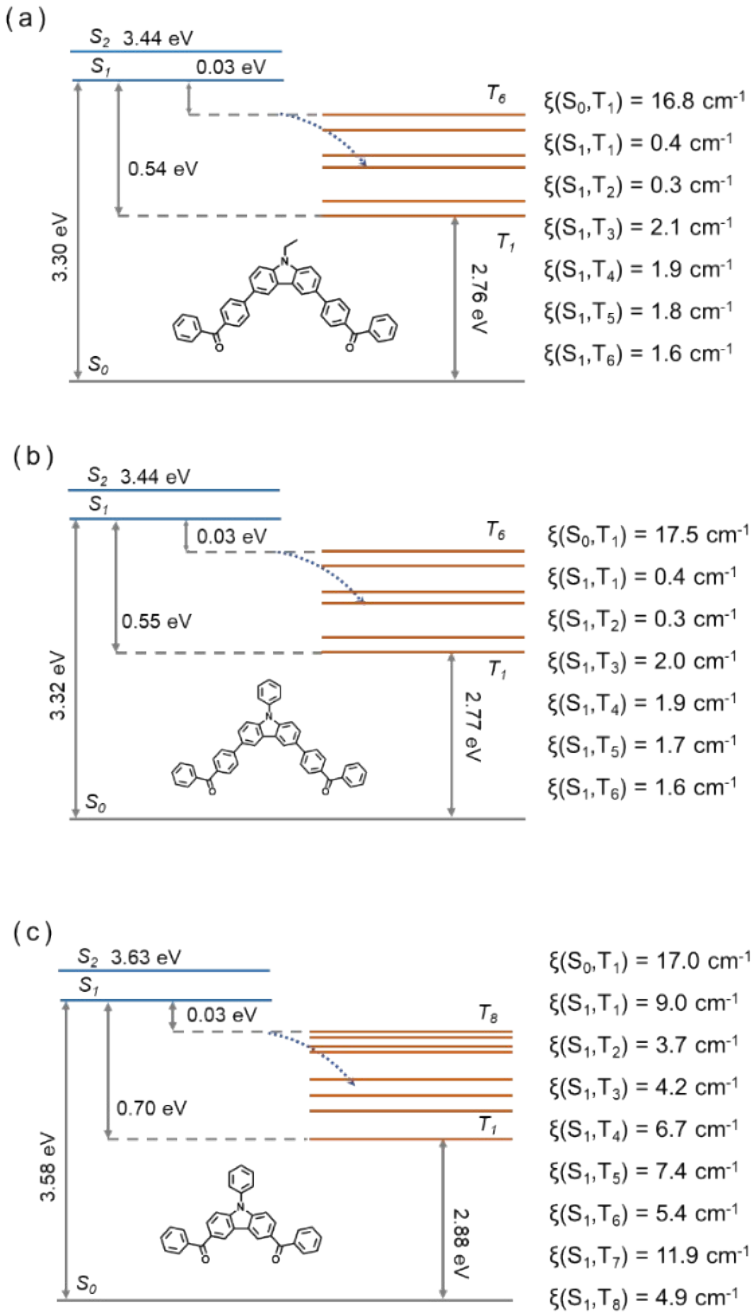

Fig. S18. The singlet (S_n) and triplet (T_n) state levels and the spin-orbit coupling constants of $S_1 \rightarrow T_n$ and $S_0 \rightarrow T_1$ for (a) EtCzBP, (b) PhCzBP and (c) PhCzPM.

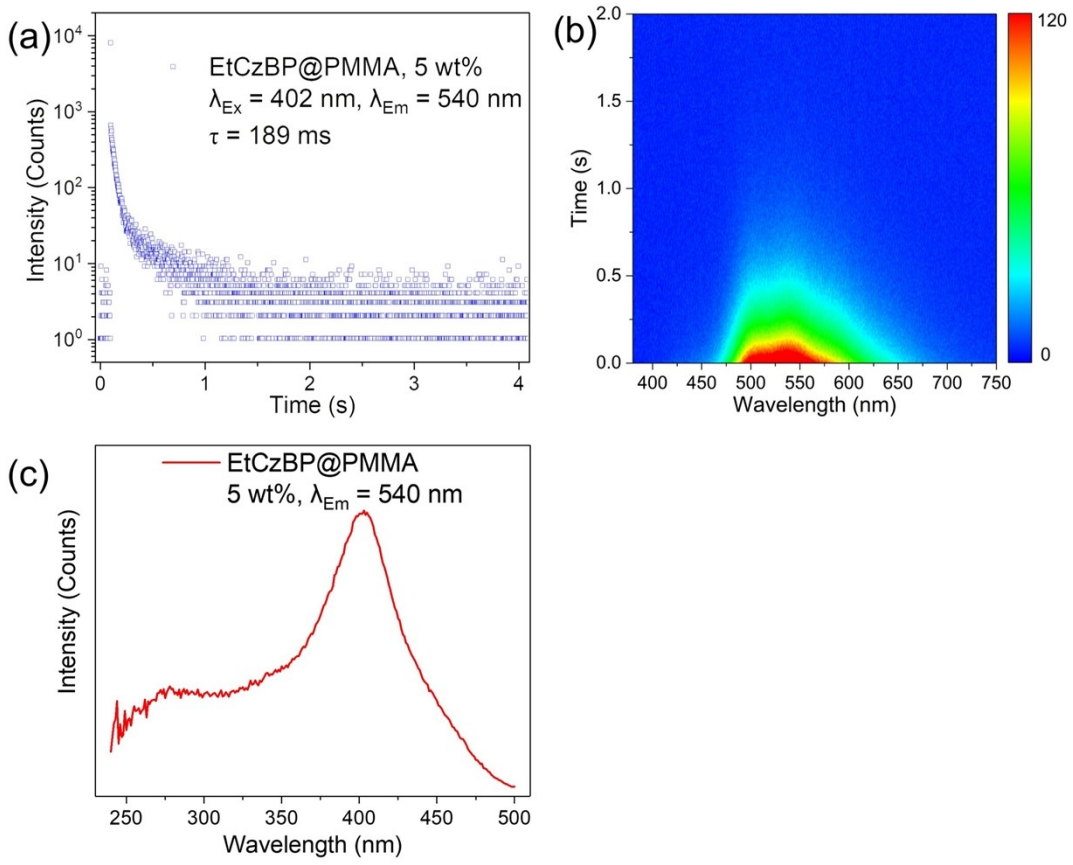

Fig. S19. Photophysical properties of EtCzBP@PMMA film with a concentration at 5 wt%. (a) Time-resolved PL-decay curves at the phosphorescence emission band of 540 nm. (τ_{int}=189±9.4 ms, X^2=1.15)(b) Transient PL decay image (delayed time = 8 ms). (c) Excitation spectrum at an emission band of 540 nm.

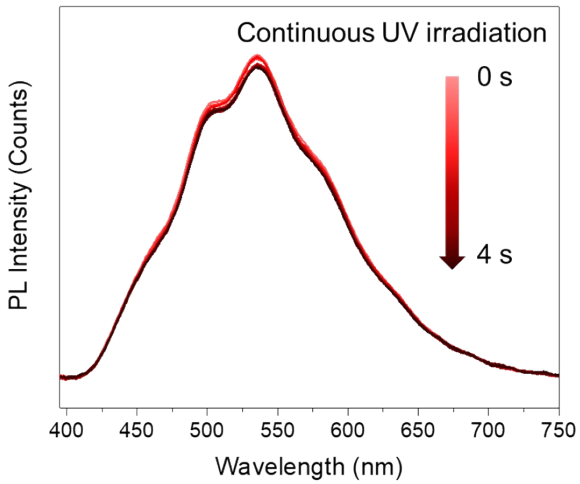

Fig. S20. Steady-state PL spectra of EtCzBP@PMMA films under sustaining UV light irradiation (λ_{ex} = 365 nm) at 77 K.

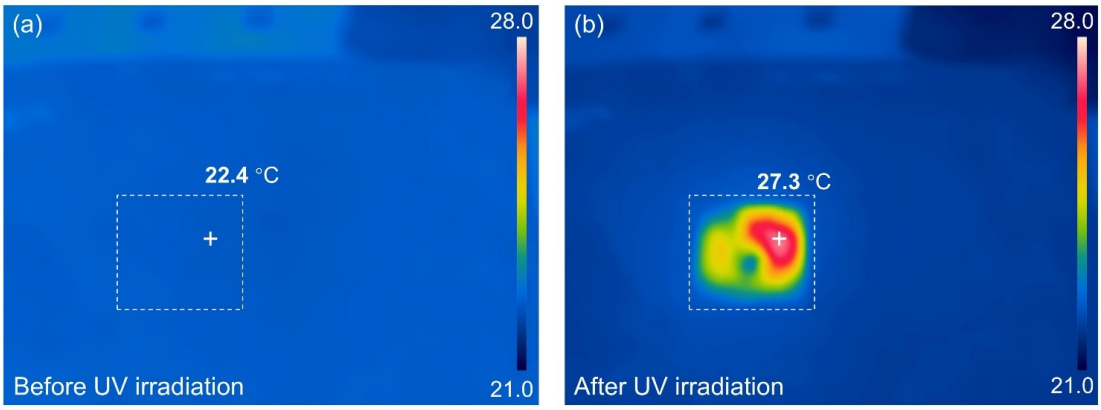

Fig. S21. Infrared images of EtCzBP@PMMA films before UV light irradiation and after sustaining UV light irradiation (λ_{ex} = 365 nm) under ambient condition.

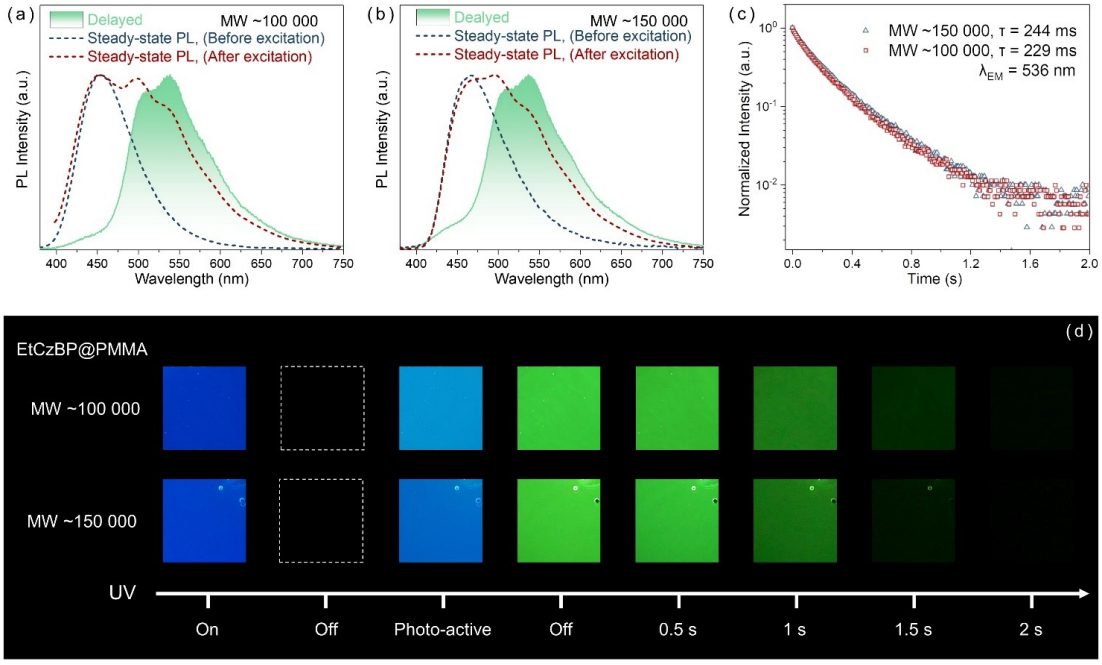

Fig. S22. The steady-state PL spectra before UV excitation and after UV excitation, and delayed (delayed time = 8 ms) spectra for EtCzBP@PMMA (The molecular weights of PMMA were ~150 000 (a) and 100 000 (b), respectively). (c) Time-resolved PL-decay curves at the phosphorescence emission band of 536 nm. (d) Photographs of the photo-active RTP of EtCzBP@PMMA with different molecular weights under the UV excitation (λ_{ex}= 365 nm).

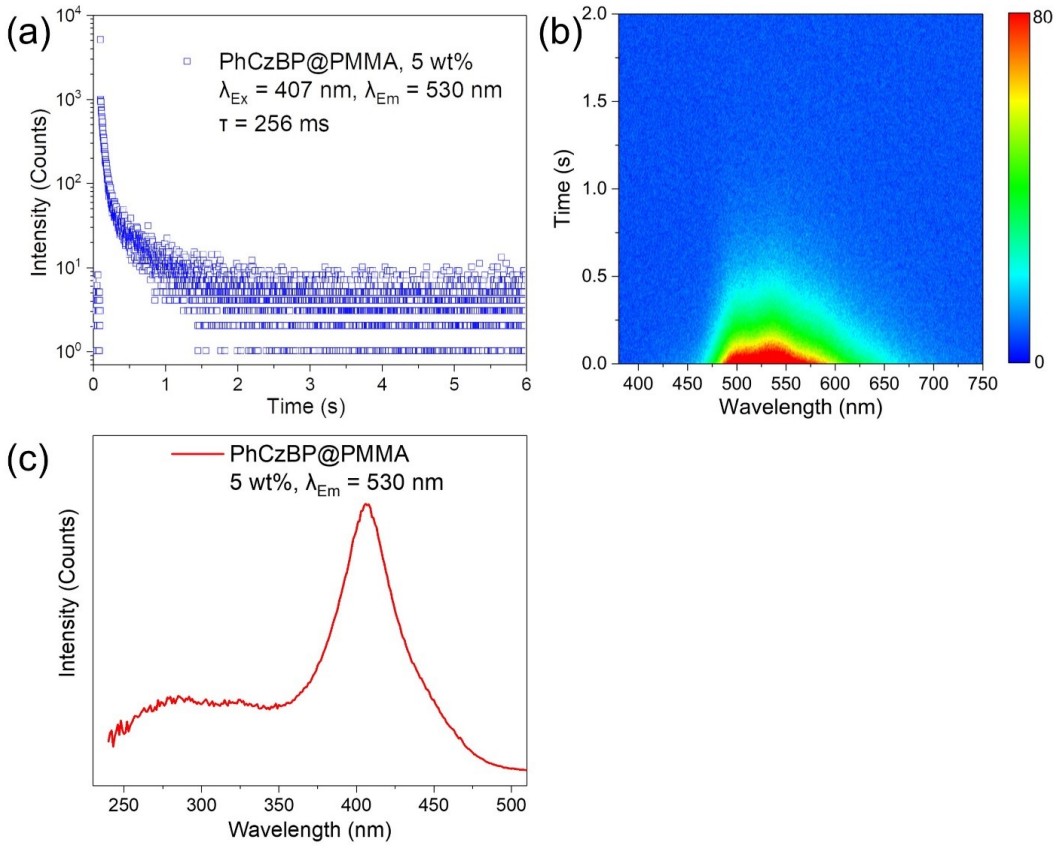

Fig. S23. Photophysical properties of PhCzBP@PMMA film with a concentration at 5 wt%. (a) Time-resolved PL-decay curves at the phosphorescence emission band of 530 nm. (τ_{int}=256±8.7 ms, X^2=1.22) (b) Transient PL decay image (delayed time =8 ms). (c) Excitation spectrum at an emission band of 540 nm.

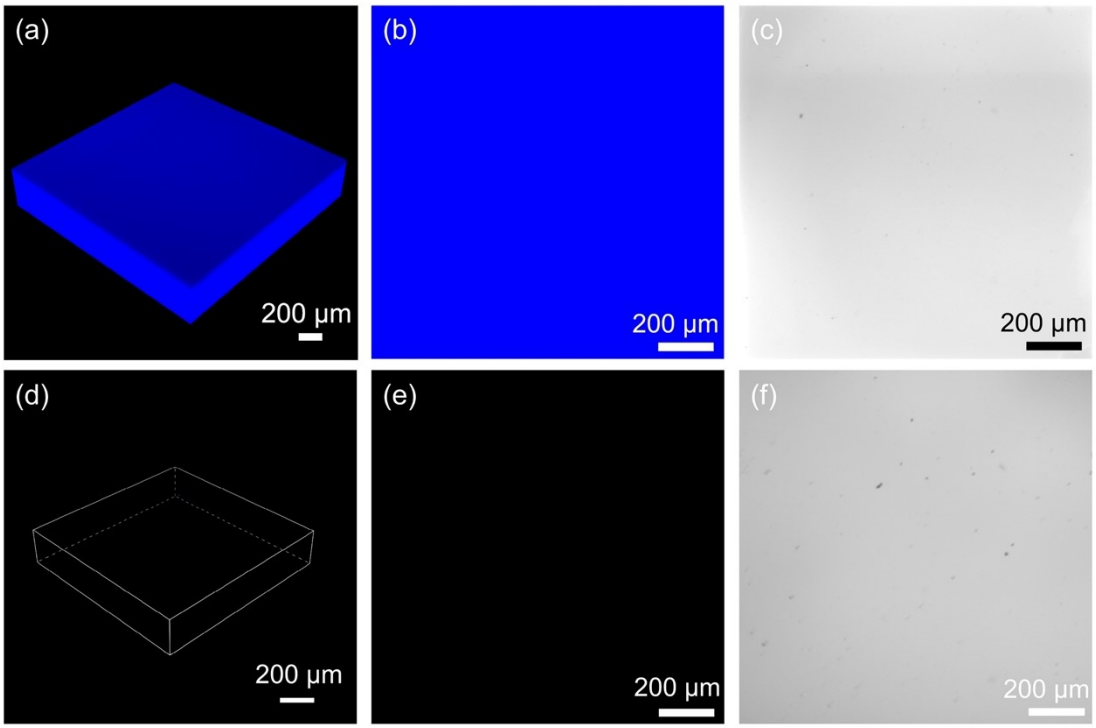

Fig. S24. Three-dimensional and planar laser scanning confocal microscopy (LSCM), and optical microscopy images of (a, b, c) EtCzBP@PMMA films and (d, e, f) pure PMMA films.

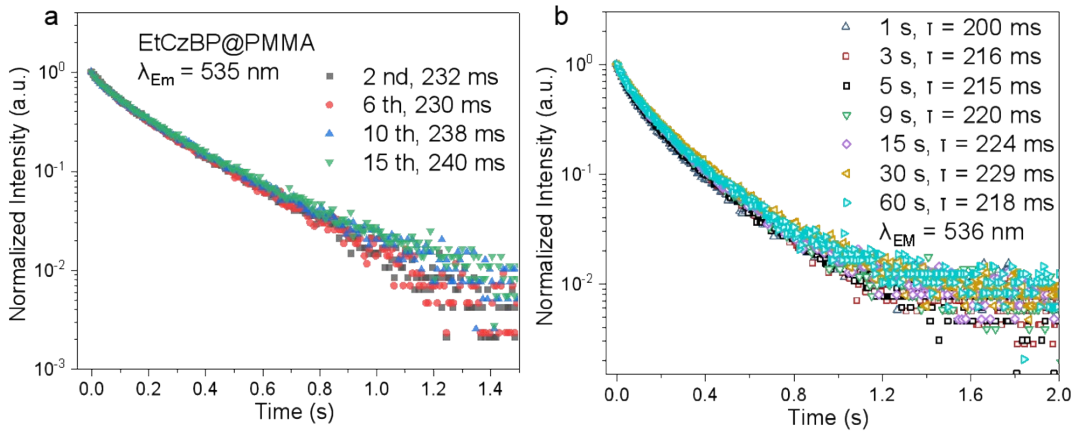

Fig. S25. Time-resolved PL-decay curves at the phosphorescent emission band of 535 nm (a) during the 2 nd, 6th, 10th, and 15th cycles of cyclic testing process. (b) different UV irradiation duration.

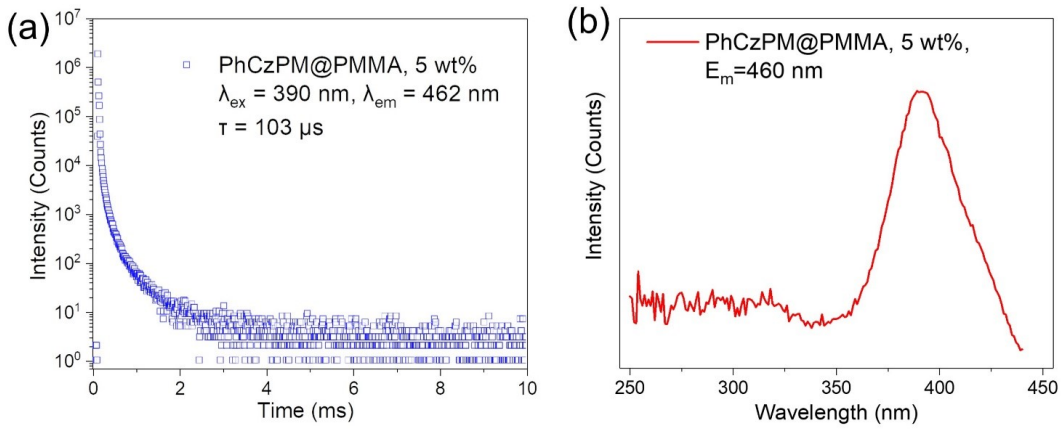

Fig. S26. Photophysical properties of PhCzPM@PMMA film with a concentration at 5 wt%. (a) Time-resolved PL-decay curves at the phosphorescence emission band of 462 nm.(τ_{int}=103±2.8μs, X^2=1.36) (b) Excitation spectrum at an emission band of 460 nm.

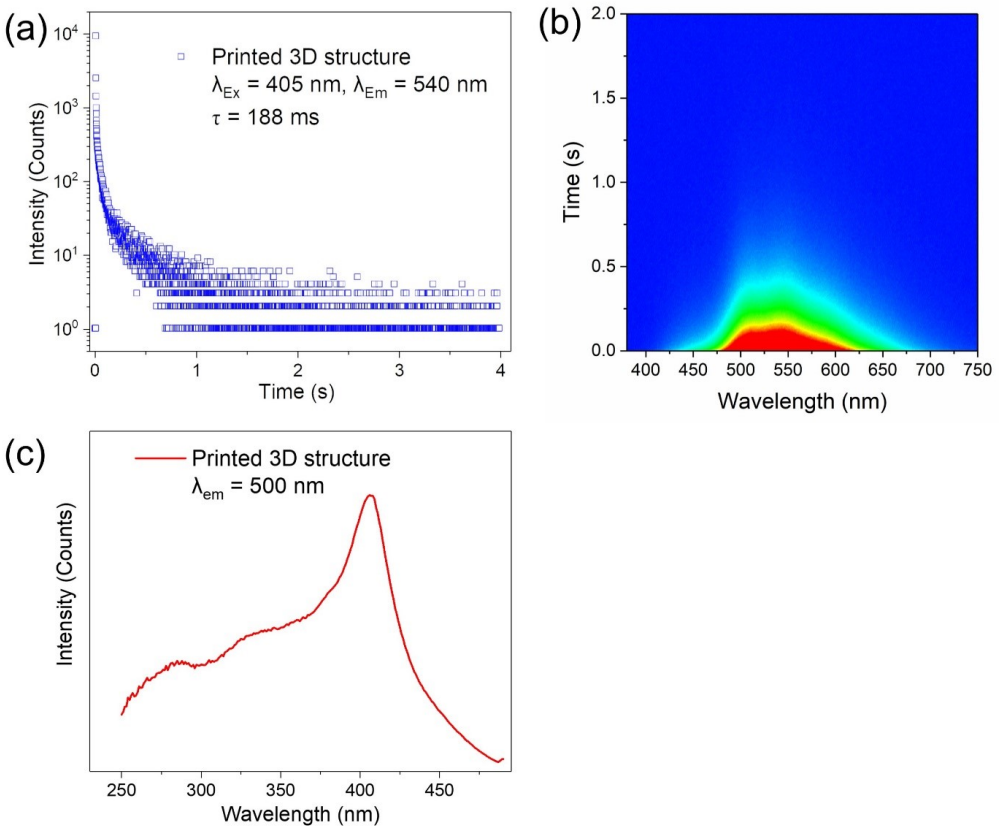

Fig. S27. Photophysical properties of printed 3D structures. (a) Time-resolved PL-decay curves at the phosphorescence emission band of 540 nm (τ_{int}=188±8.9μs,

X^2=1.10). (b) Transient PL decay image (delayed time = 8 ms). (c) Excitation spectrum at an emission band of 500 nm.

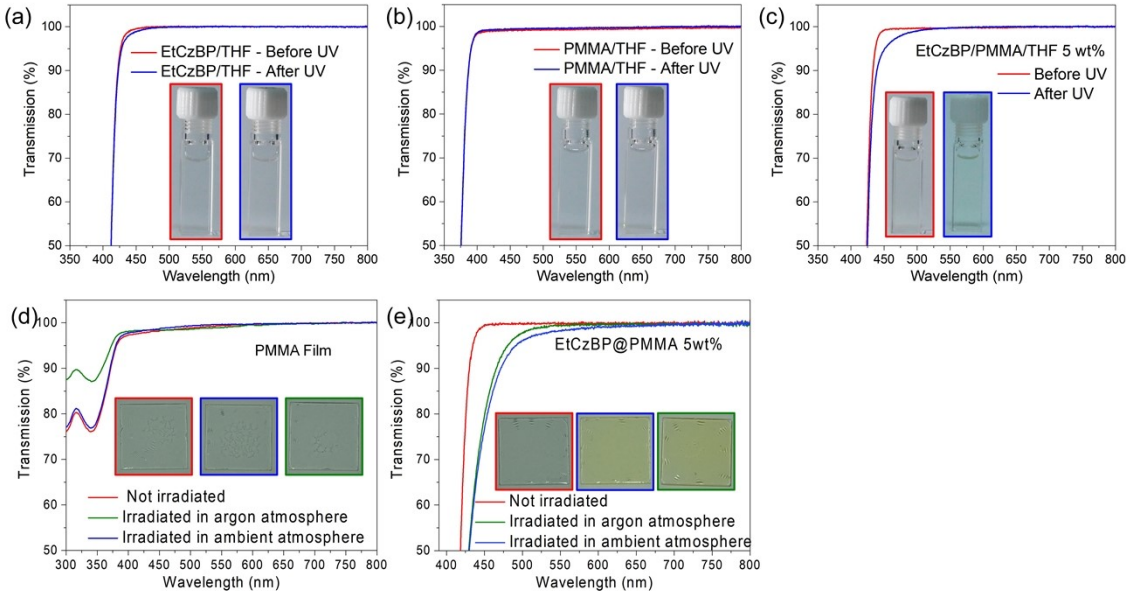

Fig. S28. Mechanisms of oxygen consumption during photoactivation. Transmission of cuvettes containing (a) EtCzBP, (b) PMMA and (c) PMMA/EtCzBP (5 wt%) in tetrahydrofuran (1×10^{-5}M) shown before and after illumination with UV light, inset: photographs of the cuvettes containing solutions. Transmission of drop casted (d) PMMA and (e) EtCzBP@PMMA (5 wt%) before illumination with UV light, and irradiation in argon and ambient atmosphere, inset: the corresponding photographs of each stage of the polymer films.

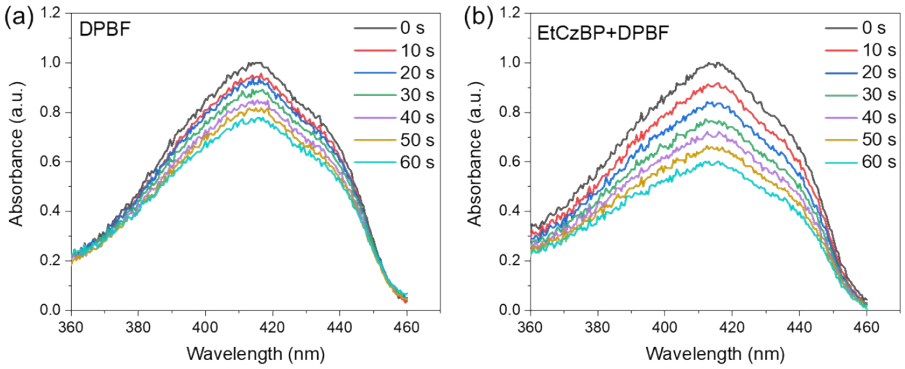

Fig. S29. Time-dependent absorbance of (a) DPBF and (b) EtCzBP&DPBF irradiated by 365 nm for various time. The absorbance of mixed solutions containing EtCzBP

and DPBF declined to 59% of their initial intensity under 365 nm photoirradiation for 60 s. In contrast, the absorbance of DPBF decreased to 77%, indicating that the triplet excitons of EtCzBP could interact with triplet oxygen through TTA process to accelerate the generation of excited singlet oxygen.

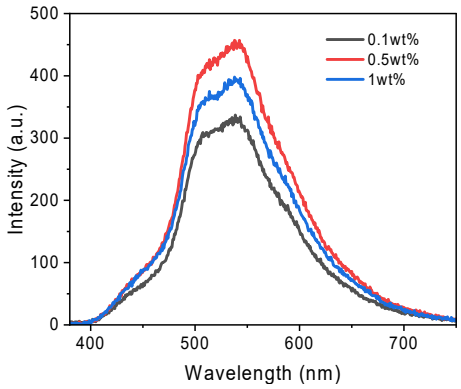

Fig. S30. Diverse RTP intensities at different doping concentrations of EtCzBP@PMMA.

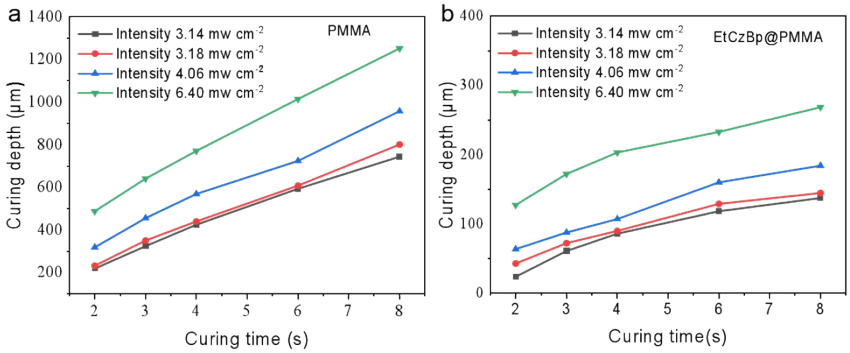

Fig. S31. The curing depth of (a)PMMA and (b)EtCzBP@PMMA (0.5 wt%) with different light source power power during the photocuring process.

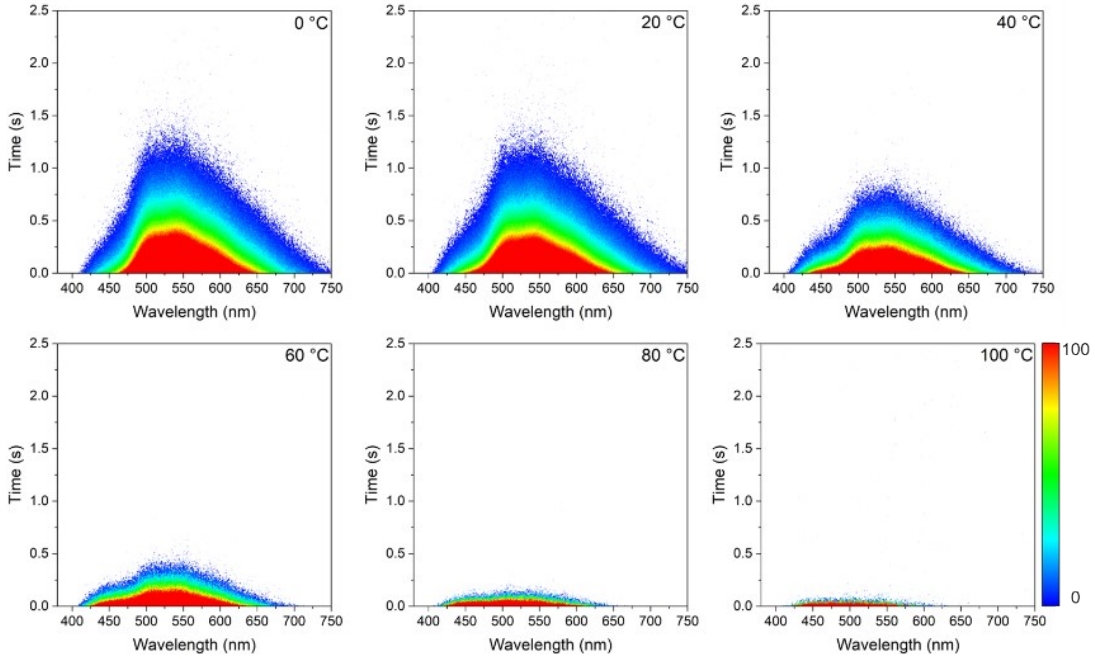

Fig. S32. Transient PL decay image (delayed time = 8 ms) for the cured printable resins at different temperatures (λ_{ex} = 365 nm).

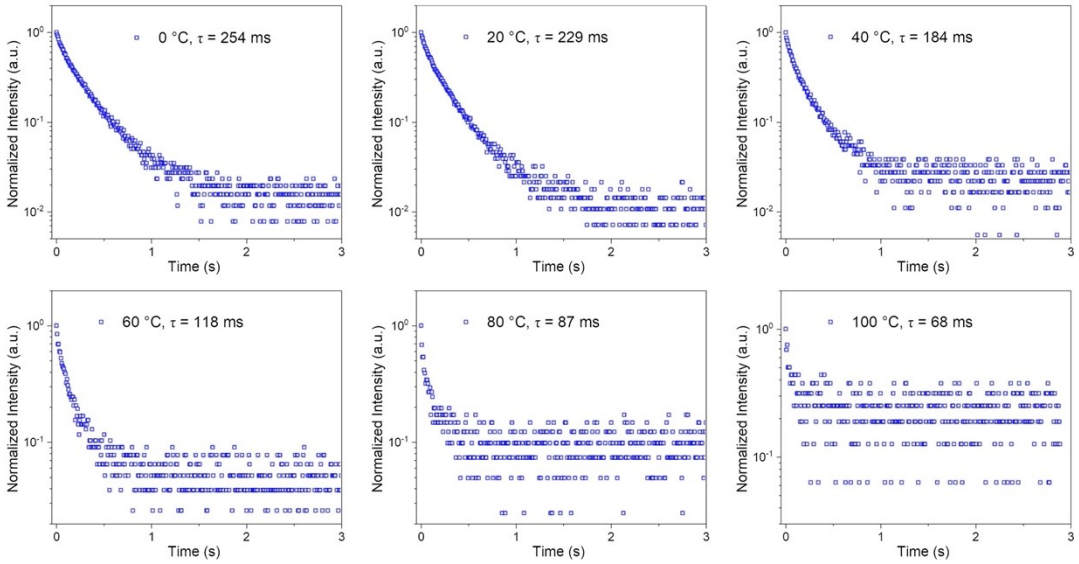

Fig. S33. Time-resolved PL-decay curves for the cured printable resins at the phosphorescence emission band of 536 nm.

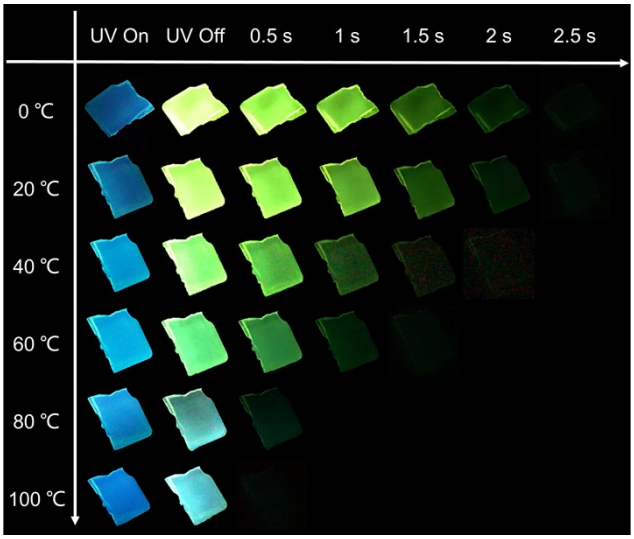

Fig. S34. Photographs of the cured printable resins under UV excitation and after termination of UV light at different temperatures.

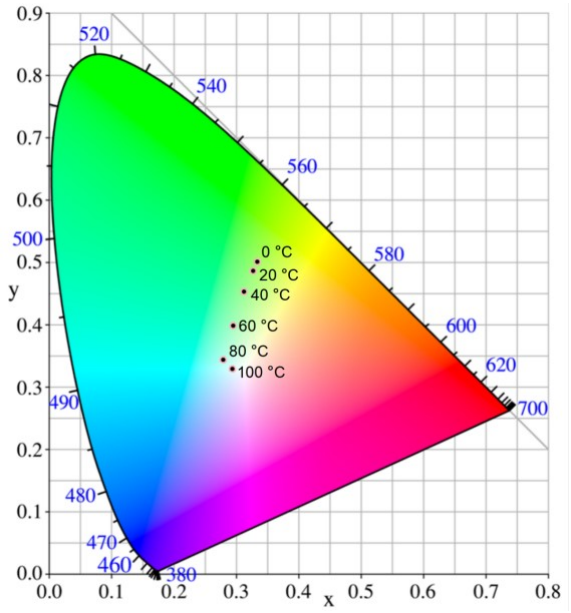

Fig. S35. CIE coordinates for the cured printable resins at different temperatures (λ_{ex} = 365 nm).

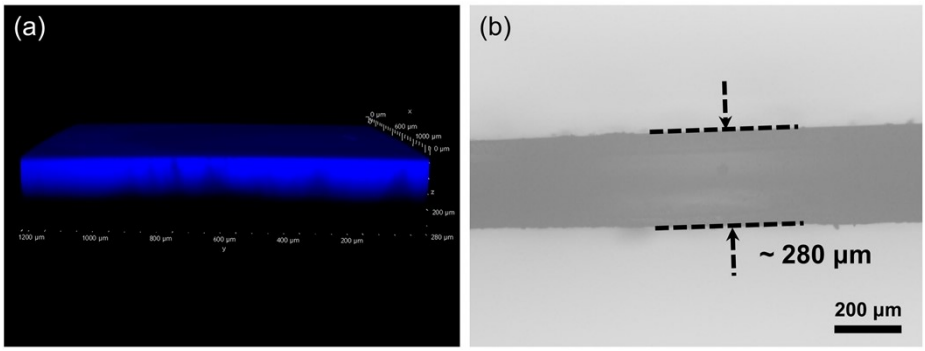

Fig. S36. (a) Three-dimensional laser scanning confocal microscopy (LSCM) under 405 nm excitation and (b) optical microscopy images of the 3D printed structures.

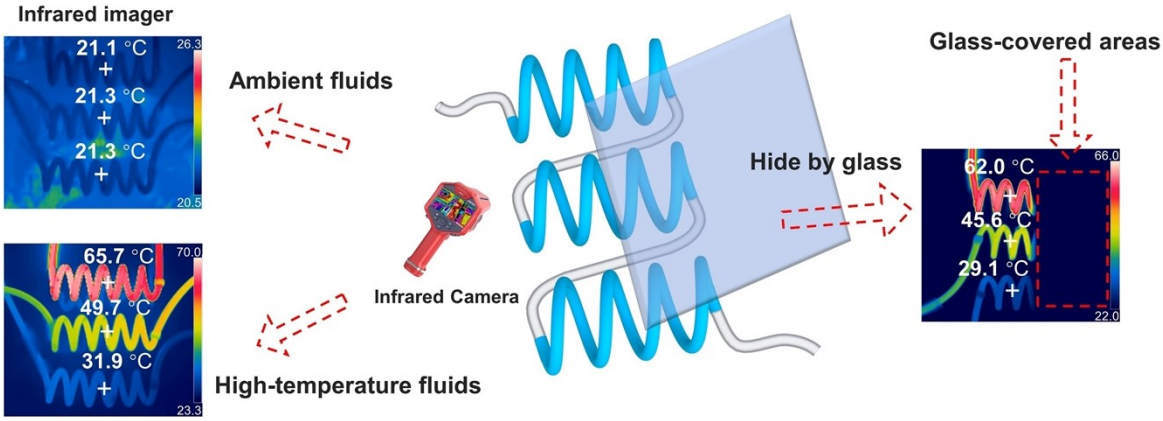

Fig. S37. Schematic diagram of the phosphorescence-based temperature real-time sensing structures transmitting temperature signals through transparent glass.

Crystal data for EtCzBP: $C_{40}H_{29}NO_2$ (M = 555.64 g/mol), orthorhombic, space group $P2_12_12_1$, a = 7.70890(10) Å, b = 24.1610(2) Å, c = 30.3400(3) Å, α = 90°, β = 90 °, γ = 90°, V = 5650.97(10) Å^3, Z = 8, T = 100.00(10) K, μ(Cu Kα) = 0.622 mm^{-1}, ρ_c = 1.306 g/cm^3, Reflections collected 38426, Independent reflections 11462 unique [R_{int} = 0.0369, R_{sigma} = 0.0355]. R_1 = 0.0345 (I > 2σ(I)) and wR_2 = 0.0895 (all data). GOF = 1.087.

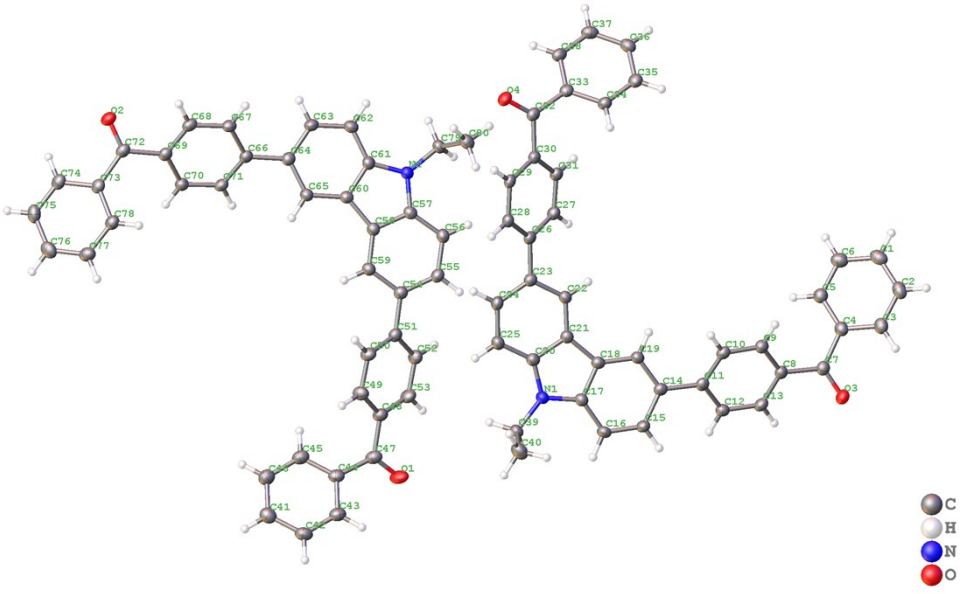

Fig. S35. Single crystal structure for EtCzBP.

Table S4. Bond distance (Å) for EtCzBP.

Atom	Atom	Length/Å	Atom	Atom	Length/Å
O4	C32	1.223(2)	C20	C25	1.398(3)
O2	C72	1.225(2)	C7	C4	1.497(3)
O3	C7	1.219(3)	C70	C69	1.402(3)
O1	C47	1.220(3)	C65	C64	1.392(3)
N2	C57	1.379(3)	C11	C14	1.480(3)
N2	C61	1.387(3)	C11	C10	1.399(3)
N2	C79	1.462(2)	C11	C12	1.409(3)
N1	C17	1.378(3)	C14	C15	1.413(3)
N1	C20	1.383(3)	C22	C21	1.388(3)
N1	C39	1.459(2)	C24	C25	1.389(3)
C58	C57	1.412(3)	C69	C68	1.389(3)
C58	C59	1.388(3)	C15	C16	1.382(3)
C58	C60	1.444(3)	C64	C66	1.482(3)
C17	C18	1.409(3)	C64	C63	1.415(3)
C17	C16	1.397(3)	C54	C55	1.410(3)
C28	C29	1.388(3)	C54	C51	1.480(3)
C28	C26	1.399(3)	C73	C78	1.396(3)
C57	C56	1.397(3)	C73	C74	1.401(3)
C18	C19	1.386(3)	C13	C12	1.381(3)
C18	C21	1.443(3)	C48	C47	1.494(3)
C32	C33	1.498(3)	C48	C49	1.395(3)
C32	C30	1.496(3)	C48	C53	1.399(3)
C67	C68	1.384(3)	C44	C47	1.502(3)
C67	C66	1.405(3)	C44	C43	1.396(3)
C33	C34	1.395(3)	C44	C45	1.395(3)
C33	C38	1.392(3)	C78	C77	1.395(3)
C71	C70	1.385(3)	C49	C50	1.385(3)
C71	C66	1.395(3)	C51	C52	1.400(3)
C8	C9	1.404(3)	C51	C50	1.397(3)
C8	C7	1.493(3)	C38	C37	1.390(3)
C8	C13	1.398(3)	C74	C75	1.386(3)
C27	C31	1.380(3)	C62	C63	1.383(3)
C27	C26	1.403(3)	C36	C35	1.386(3)
C30	C29	1.402(3)	C36	C37	1.391(3)
C30	C31	1.394(3)	C2	C3	1.390(3)

C59	C54	1.394(3)	C2	C1	1.391(3)
C23	C22	1.393(3)	C79	C80	1.512(3)
C23	C24	1.411(3)	C3	C4	1.397(3)
C23	C26	1.480(3)	C52	C53	1.380(3)
C60	C61	1.413(3)	C4	C5	1.404(3)
C60	C65	1.393(3)	C5	C6	1.390(3)
C34	C35	1.389(3)	C77	C76	1.386(3)
C72	C69	1.493(3)	C43	C42	1.385(3)
C72	C73	1.497(3)	C45	C46	1.392(3)
C19	C14	1.393(3)	C1	C6	1.386(4)
C9	C10	1.383(3)	C39	C40	1.518(3)
C61	C62	1.394(3)	C75	C76	1.387(3)
C56	C55	1.385(3)	C42	C41	1.390(3)
C20	C21	1.412(3)	C41	C46	1.388(3)

Table S5. Bond Angles for EtCzBP.

Atom	Atom	Atom	Angle/°	Atom	Atom	Atom	Angle/°
C57	N2	C61	108.76(17)	C70	C69	C72	123.14(19)
C57	N2	C79	124.09(17)	C68	C69	C72	118.14(18)
C61	N2	C79	126.98(17)	C68	C69	C70	118.66(19)
C17	N1	C20	108.74(17)	C20	C21	C18	107.09(18)
C17	N1	C39	124.23(17)	C22	C21	C18	132.90(19)
C20	N1	C39	126.74(17)	C22	C21	C20	120.00(18)
C57	C58	C60	106.33(18)	C16	C15	C14	122.67(19)
C59	C58	C57	119.91(18)	C67	C68	C69	121.03(19)
C59	C58	C60	133.6(2)	C65	C64	C66	119.89(18)
N1	C17	C18	109.67(18)	C65	C64	C63	118.92(19)
N1	C17	C16	129.44(19)	C63	C64	C66	121.19(18)
C16	C17	C18	120.90(19)	C28	C26	C27	117.41(19)
C29	C28	C26	121.20(19)	C28	C26	C23	123.09(19)
N2	C57	C58	109.34(18)	C27	C26	C23	119.42(18)
N2	C57	C56	129.40(19)	C59	C54	C55	119.20(19)
C56	C57	C58	121.22(19)	C59	C54	C51	119.55(19)
C17	C18	C21	105.91(18)	C55	C54	C51	121.21(18)
C19	C18	C17	120.36(19)	C78	C73	C72	122.95(19)
C19	C18	C21	133.73(19)	C78	C73	C74	119.2(2)
O4	C32	C33	120.68(18)	C74	C73	C72	117.82(19)
O4	C32	C30	120.69(19)	C12	C13	C8	120.67(19)
C30	C32	C33	118.58(17)	C49	C48	C47	122.74(19)

C68	C67	C66	120.83(19)	C49	C48	C53	118.15(19)
C34	C33	C32	121.28(18)	C53	C48	C47	119.07(19)
C38	C33	C32	119.04(18)	C43	C44	C47	118.0(2)
C38	C33	C34	119.67(19)	C45	C44	C47	122.67(19)
C70	C71	C66	121.66(18)	C45	C44	C43	119.2(2)
C9	C8	C7	122.82(19)	C15	C16	C17	117.61(19)
C13	C8	C9	118.51(19)	C24	C25	C20	117.99(19)
C13	C8	C7	118.53(18)	C77	C78	C73	120.0(2)
C31	C27	C26	121.61(19)	C67	C66	C64	121.35(19)
C29	C30	C32	119.71(18)	C71	C66	C67	117.67(19)
C31	C30	C32	121.65(18)	C71	C66	C64	120.97(18)
C31	C30	C29	118.30(18)	O1	C47	C48	119.6(2)
C58	C59	C54	119.77(19)	O1	C47	C44	119.8(2)
C22	C23	C24	119.07(18)	C48	C47	C44	120.67(18)
C22	C23	C26	118.69(18)	C56	C55	C54	122.21(19)
C24	C23	C26	122.23(18)	C50	C49	C48	120.6(2)
C61	C60	C58	106.74(18)	C52	C51	C54	121.98(19)
C65	C60	C58	133.33(19)	C50	C51	C54	120.31(18)
C65	C60	C61	119.90(19)	C50	C51	C52	117.65(19)
C35	C34	C33	120.40(19)	C13	C12	C11	121.4(2)
O2	C72	C69	119.74(19)	C37	C38	C33	120.0(2)
O2	C72	C73	119.87(19)	C75	C74	C73	120.6(2)
C69	C72	C73	120.38(17)	C63	C62	C61	118.27(19)
C18	C19	C14	119.87(19)	C35	C36	C37	120.5(2)
C10	C9	C8	120.35(19)	C3	C2	C1	119.8(2)
C28	C29	C30	120.66(18)	N2	C79	C80	112.34(18)
C27	C31	C30	120.77(19)	C36	C35	C34	119.5(2)
N2	C61	C60	108.81(18)	C2	C3	C4	120.4(2)
N2	C61	C62	130.32(19)	C53	C52	C51	121.0(2)
C62	C61	C60	120.85(19)	C62	C63	C64	122.03(19)
C55	C56	C57	117.62(19)	C49	C50	C51	121.43(19)
N1	C20	C21	108.56(17)	C3	C4	C7	118.19(19)
N1	C20	C25	130.59(19)	C3	C4	C5	119.4(2)
C25	C20	C21	120.84(19)	C5	C4	C7	122.35(19)
O3	C7	C8	120.02(19)	C6	C5	C4	119.7(2)
O3	C7	C4	120.03(19)	C52	C53	C48	121.1(2)
C8	C7	C4	119.95(18)	C76	C77	C78	119.9(2)
C71	C70	C69	120.10(19)	C42	C43	C44	120.4(2)
C64	C65	C60	120.02(19)	C46	C45	C44	120.2(2)
C10	C11	C14	121.34(18)	C38	C37	C36	119.8(2)
C10	C11	C12	117.31(19)	C6	C1	C2	120.2(2)

C12	C11	C14	121.32(19)	N1	C39	C40	112.33(19)
C19	C14	C11	120.69(18)	C74	C75	C76	119.6(2)
C19	C14	C15	118.58(19)	C43	C42	C41	120.4(2)
C15	C14	C11	120.71(18)	C77	C76	C75	120.6(2)
C21	C22	C23	120.07(19)	C1	C6	C5	120.4(2)
C9	C10	C11	121.69(19)	C46	C41	C42	119.6(2)
C25	C24	C23	121.99(19)	C41	C46	C45	120.3(2)

Crystal data for PhCzBP: $C_{44}H_{29}NO_2$ (M = 603.68 g/mol), monoclinic, space group $P2_1/c$, a = 15.739(2) Å, b = 16.068(2) Å, c = 13.9254(19) Å, α = 90°, β = 107.433(2) °, γ = 90°, V = 3359.9(8) $Å^3$, Z = 4, T = 296.15 K, μ(MoKα) = 0.072 mm^{-1}, ρ_c = 1.193 g/cm^3, Reflections collected 19309, Independent reflections 7549 unique [R_{int} = 0.0675, R_{sigma} = 0.1083]. R_1 = 0.0791 (I > 2σ(I)) and wR_2 = 0.2976 (all data). GOF = 0.936.

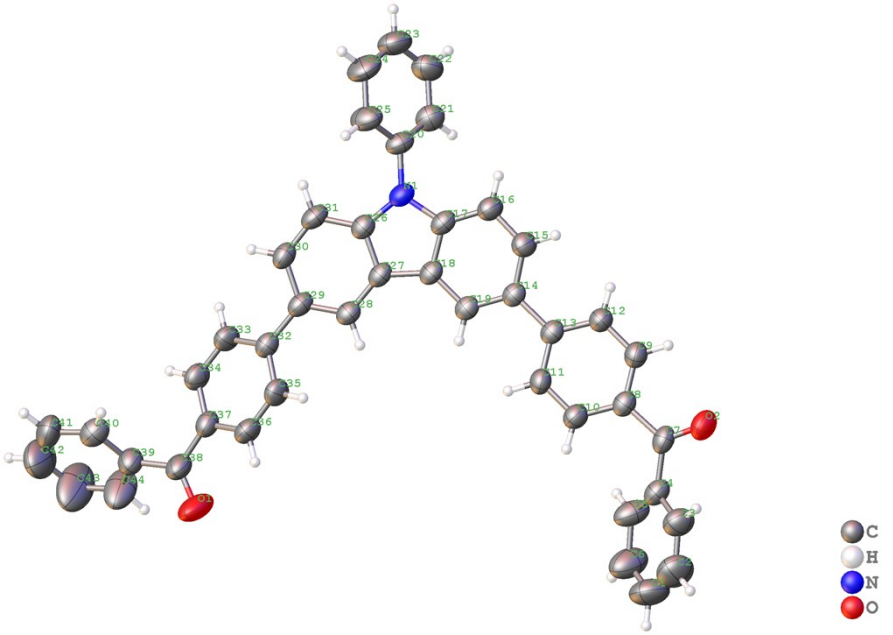

Fig. S36. Single crystal structure for PhCzBP.

Table S6. Bond distance (Å) for PhCzBP.

Atom	Atom	Length/Å	Atom	Atom	Length/Å
N1	C17	1.391(4)	C37	C34	1.397(5)
N1	C26	1.396(4)	C37	C36	1.396(5)
N1	C20	1.425(4)	C37	C38	1.477(5)
O2	C7	1.232(4)	C20	C21	1.381(5)
C18	C27	1.440(5)	C20	C25	1.371(5)
C18	C19	1.395(5)	C15	C16	1.373(5)
C18	C17	1.414(5)	C31	C30	1.368(5)
C14	C19	1.388(5)	C4	C3	1.369(6)
C14	C13	1.485(5)	C4	C5	1.386(6)
C14	C15	1.408(5)	C33	C34	1.374(5)
C27	C28	1.389(5)	O1	C38	1.222(5)
C27	C26	1.397(5)	C35	C36	1.373(5)
C8	C7	1.482(5)	C21	C22	1.377(5)
C8	C10	1.389(5)	C39	C38	1.482(6)
C8	C9	1.382(5)	C39	C40	1.369(6)
C13	C11	1.397(5)	C39	C44	1.372(6)
C13	C12	1.386(5)	C3	C2	1.350(6)
C28	C29	1.370(5)	C40	C41	1.388(6)
C17	C16	1.381(5)	C25	C24	1.383(6)
C26	C31	1.395(5)	C22	C23	1.361(7)
C32	C29	1.483(5)	C5	C6	1.378(6)
C32	C33	1.394(5)	C23	C24	1.371(7)
C32	C35	1.395(5)	C41	C42	1.370(8)
C29	C30	1.412(5)	C2	C1	1.373(8)
C11	C10	1.378(5)	C6	C1	1.367(9)
C7	C4	1.463(5)	C44	C43	1.383(9)
C12	C9	1.377(5)	C42	C43	1.359(9)

Table S7. Bond Angles for PhCzBP.

Atom	Atom	Atom	Angle/°	Atom	Atom	Atom	Angle/°
C17	N1	C26	108.0(3)	C36	C37	C34	117.7(3)
C17	N1	C20	125.7(3)	C36	C37	C38	119.3(4)
C26	N1	C20	126.1(3)	C21	C20	N1	119.9(3)
C19	C18	C27	133.3(3)	C25	C20	N1	119.7(4)
C19	C18	C17	119.8(3)	C25	C20	C21	120.3(4)
C17	C18	C27	106.8(3)	C16	C15	C14	123.7(3)
C19	C14	C13	121.0(3)	C30	C31	C26	118.0(3)
C19	C14	C15	117.5(3)	C12	C9	C8	121.6(4)
C15	C14	C13	121.5(3)	C31	C30	C29	122.7(3)

C28	C27	C18	133.1(3)	C3	C4	C7	118.3(4)
C28	C27	C26	120.0(3)	C3	C4	C5	118.6(4)
C26	C27	C18	106.9(3)	C5	C4	C7	123.0(4)
C14	C19	C18	120.4(3)	C15	C16	C17	117.9(3)
C10	C8	C7	123.4(3)	C34	C33	C32	122.2(4)
C9	C8	C7	119.2(3)	C33	C34	C37	120.5(4)
C9	C8	C10	117.4(3)	C36	C35	C32	121.8(4)
C11	C13	C14	121.4(3)	C22	C21	C20	119.3(4)
C12	C13	C14	122.2(3)	C35	C36	C37	121.1(4)
C12	C13	C11	116.3(3)	C40	C39	C38	122.5(4)
C29	C28	C27	120.6(3)	C40	C39	C44	118.3(4)
N1	C17	C18	108.8(3)	C44	C39	C38	119.0(4)
C16	C17	N1	130.6(3)	C37	C38	C39	121.6(4)
C16	C17	C18	120.6(3)	O1	C38	C37	119.3(4)
N1	C26	C27	109.5(3)	O1	C38	C39	119.0(4)
C31	C26	N1	130.1(3)	C2	C3	C4	121.7(5)
C31	C26	C27	120.5(3)	C39	C40	C41	120.5(5)
C33	C32	C29	122.5(3)	C20	C25	C24	119.3(4)
C33	C32	C35	116.7(3)	C23	C22	C21	121.0(5)
C35	C32	C29	120.8(3)	C6	C5	C4	119.9(5)
C28	C29	C32	120.9(3)	C22	C23	C24	119.5(4)
C28	C29	C30	118.2(3)	C23	C24	C25	120.6(5)
C30	C29	C32	120.8(3)	C42	C41	C40	120.0(5)
C10	C11	C13	122.0(3)	C3	C2	C1	119.9(5)
O2	C7	C8	119.4(4)	C1	C6	C5	120.1(6)
O2	C7	C4	117.4(3)	C6	C1	C2	119.9(5)
C4	C7	C8	123.2(3)	C39	C44	C43	121.6(6)
C11	C10	C8	120.8(3)	C43	C42	C41	120.2(6)
C9	C12	C13	121.8(3)	C42	C43	C44	119.3(6)
C34	C37	C38	122.9(4)				

Crystal data for PhCzPM: $C_{33}H_{23}Cl_2NO_2$ (M = 536.42 g/mol), monoclinic, space group $P2_1/c$, a = 12.8697(6) Å, b = 26.1356(9) Å, c = 7.9805(3) Å, α = 90°, β = 107.143(4) °, γ = 90°, V = 2565.04(18) Å^3, *Z* = 4, T = 100.00(10) K, μ(Mo Kα) = 0.286 mm^{-1}, ρ_c = 1.389 g/cm^3, Reflections collected 16607, Independent reflections 5587 unique [R_{int} = 0.0310, R_{sigma} = 0.0411]. R_1 = 0.0589 (I > 2σ(I)) and wR_2 = 0.1832 (all data). GOF = 1.057.

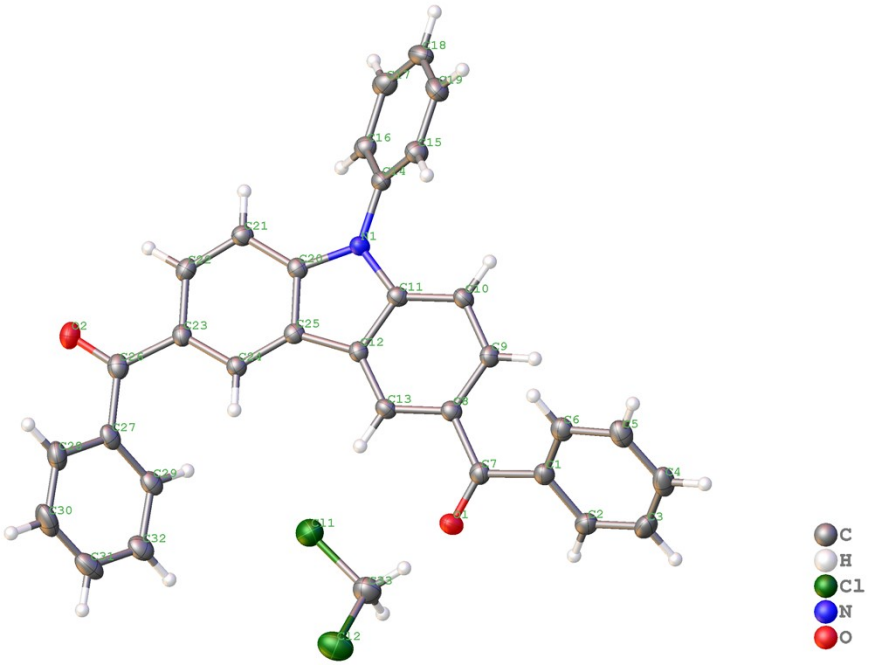

Fig. S37. Single crystal structure for PhCzPM.

Table S8. Bond distance (Å) for PhCzPM.

Atom	Atom	Length/Å	Atom	Atom	Length/Å
Cl1	C33	1.769(3)	C9	C10	1.390(3)
Cl2	C33	1.765(3)	C8	C7	1.490(3)
O1	C7	1.226(3)	C23	C26	1.488(4)
O2	C26	1.228(3)	C7	C1	1.496(4)
N1	C20	1.388(3)	C2	C1	1.395(4)
N1	C11	1.393(3)	C2	C3	1.380(4)
N1	C14	1.435(3)	C27	C29	1.388(4)
C20	C25	1.409(3)	C27	C26	1.503(4)
C20	C21	1.406(3)	C27	C28	1.401(4)
C13	C12	1.388(3)	C1	C6	1.394(4)
C13	C8	1.395(4)	C16	C17	1.383(4)
C25	C12	1.447(3)	C29	C32	1.395(4)
C25	C24	1.388(4)	C6	C5	1.390(4)
C12	C11	1.418(3)	C15	C19	1.384(4)
C11	C10	1.393(4)	C19	C18	1.393(4)
C14	C16	1.396(3)	C32	C31	1.383(4)
C14	C15	1.385(4)	C5	C4	1.379(4)
C24	C23	1.399(3)	C3	C4	1.393(5)
C21	C22	1.375(4)	C17	C18	1.390(4)

C22	C23	1.418(3)	C28	C30	1.385(4)
C9	C8	1.412(4)	C31	C30	1.381(5)

Table S9. Bond Angles for PhCzPM.

Atom	Atom	Atom	Angle/°	Atom	Atom	Atom	Angle/°
C20	N1	C11	108.2(2)	C22	C23	C26	117.7(2)
C20	N1	C14	126.5(2)	O1	C7	C8	121.2(2)
C11	N1	C14	125.1(2)	O1	C7	C1	119.4(2)
N1	C20	C25	109.8(2)	C8	C7	C1	119.4(2)
N1	C20	C21	129.4(2)	C3	C2	C1	119.6(3)
C21	C20	C25	120.8(2)	C29	C27	C26	122.9(2)
C12	C13	C8	119.5(2)	C29	C27	C28	119.7(3)
C20	C25	C12	106.3(2)	C28	C27	C26	117.4(2)
C24	C25	C20	120.6(2)	C2	C1	C7	118.2(2)
C24	C25	C12	133.1(2)	C6	C1	C7	122.2(2)
C13	C12	C25	133.6(2)	C6	C1	C2	119.6(2)
C13	C12	C11	119.5(2)	C17	C16	C14	119.4(3)
C11	C12	C25	106.9(2)	C27	C29	C32	120.2(3)
N1	C11	C12	108.8(2)	O2	C26	C23	120.9(2)
C10	C11	N1	129.2(2)	O2	C26	C27	118.2(2)
C10	C11	C12	121.9(2)	C23	C26	C27	120.9(2)
C16	C14	N1	119.7(2)	C5	C6	C1	120.0(3)
C15	C14	N1	119.6(2)	C19	C15	C14	119.5(2)
C15	C14	C16	120.7(2)	C15	C19	C18	120.3(3)
C25	C24	C23	119.2(2)	C31	C32	C29	119.7(3)
C22	C21	C20	117.7(2)	C4	C5	C6	120.4(3)
C21	C22	C23	122.4(2)	C2	C3	C4	120.9(3)
C10	C9	C8	121.7(2)	C16	C17	C18	120.2(2)
C13	C8	C9	119.9(2)	C17	C18	C19	119.9(2)
C13	C8	C7	118.3(2)	C30	C28	C27	119.5(3)
C9	C8	C7	121.7(2)	C5	C4	C3	119.4(3)
C9	C10	C11	117.5(2)	C30	C31	C32	120.2(3)
C24	C23	C22	119.1(2)	C31	C30	C28	120.6(3)
C24	C23	C26	123.1(2)	Cl2	C33	Cl1	112.27(18)

References

1. H. Sun, Z. Xie, H. Wang, Y. Wu, B. Du, C. Guan and T. Yu, *J. Mater.Chem. C*, 2022, **10**, 8854-8859.
2. D. Gudeika, J. Vidas Grazulevicius, D. Volyniuk, R. Butkute, G. Juska , A. Miasojedovas, A. Gruodis, S. Jursenas, *Dyes Pigm.*, 2015, **114**, 239-252.
3. X.-F. Zhang and X. Li, *J. Lumin.*, 2011, **131**, 2263-2266.
4. D. Liu, M. Zhang, W. Tian, W. Jiang, Y. Sun, Z. Zhao and B. Z. Tang, *Aggregate*, 2022, **3**, e164.
5. C. Liu, Y. Cao, Y. Cheng, D. Wang, T. Xu, L. Su, X. Zhang and H. Dong, *Nat. Commun.*, 2020, **11**, 1735.
6. C. Lee, W. Yang and R. G. Parr, *Phys. Rev. B*, 1988, **37**, 785-789.
7. P. J. Stephens, F. J. Devlin, C. F. Chabalowski and M. J. Frisch, *J. Chem. Phys.*, 1994, **98**, 11623-11627.
8. F. Neese, *WIREs Computational Molecular Science*, 2018, **8**, e1327.
9. T. Lu and F. Chen, *J. Comput. Chem.*, 2012, **33**, 580-592.
10. Z. Liu, T. Lu and Q. Chen, *Carbon*, 2020, **165**, 461-467.
11. W. Humphrey, A. Dalke and K. Schulten, *J. Mol. Graph.*, 1996, **14**, 33-38.